A deeper look; Does Heincke´s law apply to Atlantic cod (*Gadus morhua*) in the Barents Sea and what is the effect of eye size on prey encounter rate?

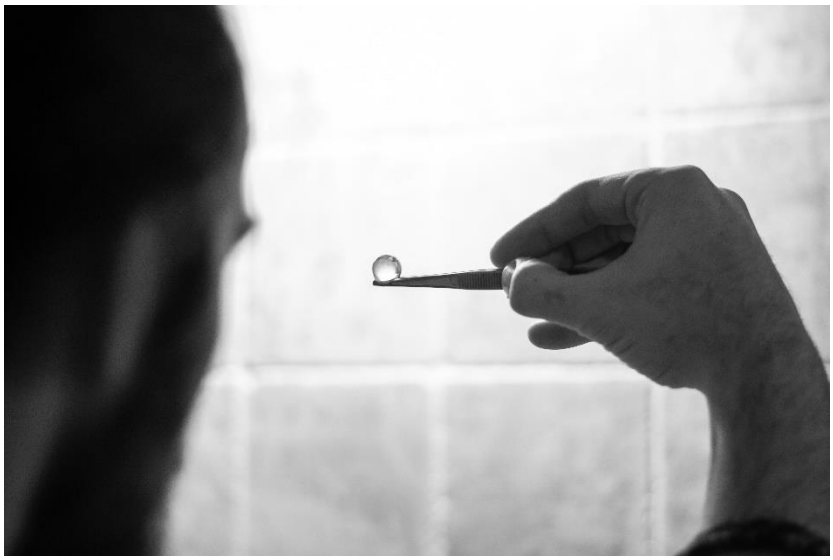

UNIVERSITETET I BERGEN
Det matematisk-naturvitenskapelige fakultet

Master of Science in Marine Biology
Department of Biology, University of Bergen

Terje Alming
May 2019

Supervisors:

Edda Johannesen, Dr. Scient., Senior researcher at Institute of Marine Research, Bergen.
Øyvind Fiksen, Dr. Scient., Professor Biological Oceanography, University of Bergen.

Acknowledments

I would like to thank Edda Joahnnesen (IMR) and Øyvind Fiksen (UiB) for being great supervisors and having shown extraordinary levels of understanding throughout this thesis. I could not have done it without them.

Great appreciation goes out to everyone at IMR and UiB whom I have contacted and have replied quickly with all the information I have requested (and then some.)

A great thanks goes out to family and friends, for supplying much needed breaks here and there.

Last but not least, I would like to thank my fiancée, Fiona Franklin, who has been supportive and caring when I needed it and inspired me to push through long days and into the night. I would never have got to where I am today without her.

Bærum

May, 2019

Terje Alming

Abstract

The Atlantic cod (*Gadus morhua*) is arguably one of the most valuable fish we have, and the Barents Sea stock, Northeast Arctic cod (NEAC), is the largest stock in the world. Despite the long history of fishing and the substantial amount of research conducted on this stock, there are still age-related aspects to the NEAC that we do not fully comprehend and no one has looked at how depth distribution changes with increasing age for this stock, a phenomenon known as ontogenetic deepening or Heincke`s law. The aims of this study are: 1) Investigate whether Heincke´s law applies to the NEAC. 2) Parameterize a model to investigate how visual range and prey encounter rate changes with cod size and depth. 3) Determine whether increased prey encounter rates as a consequence of increased visual range in larger cod can compensate for the increased energy needs associated with larger sizes. 13 years of data (2003-2016) on depth-of-capture from the joint Norwegian-Russian ecosystem surveys (BESS) was analyzed to establish average depth for different NEAC length groups. Measurements of lens size were taken from 21 cod heads acquired from a local fish shop and correlated to body size. The effect lens size would have on visual range, encounter rates and net energy balance was predicted using a visual range model. The NEAC showed a significant deepening between length groups, indicating that Heincke´s law applies to this stock. Increased lens size was predicted to increase visual range *ceteris paribus*. The positive effect increased lens size had on visual range was not sufficient to compensate for loss of light at the greater depths experienced by the larger individuals however. Additional hypotheses trying to explain Heincke´s law in other areas of the Atlantic or different species have been discussed. This thesis´ inability to explain what drives ontogenetic deepening in the NEAC goes to show the importance of understanding the intricate relationships between physical and biological factors and how they together can shape distributions.

Table of Contents

1. Introduction

1.1 Atlantic Cod

The Atlantic cod (*Gadus morhua*) is arguably one of the most valuable fish in the world, with global landings in 2016 of just over 1.3 million tons (FAO, 2018) and has been an important commodity throughout Western history. Air dried cod enabled the Vikings to roam the Atlantic and discover new lands (Kurlansky, 1999.) Salt-cured cod allowed the medieval Basques to cover great distances looking for whales while also suppling a vast international cod market. Atlantic cod has been responsible for several wars between fishing nations stretching back to the 1500's and the species´ significance can be seen in the naming of places (Cape Cod, USA and Codfish Island, New Zealand) and other, unrelated fish species (blue cod, potato cod and sleepy cod.)

Because of Atlantic cod´s global economic importance, a great deal of research has been done on this species to better understand it. In Norway its historical and economical value was made abundantly clear in 2017 when the new 200 NOK bill honored the Atlantic cod by having it as a prominent feature. And it is easy to see why it was chosen. The Barents Sea is home to the world's largest stocks of Atlantic cod, known as the Northeast Arctic Cod; or NEAC and Norway caught 378 000 tons (~44% of the total NEAC quota for the Barents Sea) in 2015 (Bakketeig, Hauge and Kvamme, 2017.) We know a great deal about how the development through different life stages (ontogeny) influences preferences with regards to temperature (Galloway, Kjørsvik and Kryvi, 1998; Ottersen, Michaelsen and Nakken, 1998), diet (Dalpadado and Bogstad, 2004; Johannesen, Johansen and Kursbrekke, 2015; Yaragina, Bogstad and Kovalev, 2009) and seasonal migrations (Jakobsen and Ozhigin, 2011, p. 230; Olsen *et al*., 2009). Despite the long history of fishing and the substantial amount of research conducted on this stock, there are still age-related aspects to the NEAC that we do not fully comprehend and no one has looked at how depth distribution changes with increasing age for this stock, a phenomenon known as ontogenetic deepening or Heincke`s law.

1.2 What is Heincke`s Law?

The history of ontogenetic deepening started in the early 1900´s with European plaice (*Pleuronectes platessa*) when the German researcher Friedrich Heincke discovered a relationship between size and average offshore distance for this species (Heincke, 1913.) He

noted that as distance from shore and depth increased, so did the average size of the fish. Heincke proposed there had to be some sort of ontogenetic driver for this pattern but did not manage to explain it further.

Since then, the increase in average size with depth has been observed in several marine fish species (Frank, 2018; Gibson *et al.,* 2002; Polloni *et al.*, 1979; Snelgrove and Haedrich, 1985) and the pattern became known as Heincke´s law. The pattern is surprisingly prevalent world-wide. A significant deepening with size has been demonstrated for at least 27 fish species in the Southeast Atlantic and 23 species in the Northwest Mediterranean (Macpherson and Duarte, 1991). Surveys done in the Algerian Basin found a bigger-deeper pattern in at least two fish communities (Moranta *et al.*, 1998) and it has been reported in rock pools in the United States (Power, 1984; Gorman, 1987; Harvey and Stewart, 1991).

So what could drive such a ubiquitous pattern? Several hypotheses have been suggested, ranging from physical to ecological explanations and they vary with species and geographical location. Predator avoidance has been linked to ontogenetic deepening in Atlantic cod in the Northwest Atlantic (Linehan, Gregory and Schneider, 2001) and flatfish in the North Pacific (Ryer, Laurel and Stoner, 2010). Shallower depths often imply more topographical diversity and macroalgae growth, which provides smaller fish with more places to hide from predators. Mortality rates usually decrease with increasing body size as the number of potential predators diminish, making predation less important as an animal grows larger (Sogard, 1997). Competition has also been suggested as a driver for Heincke´s law in Atlantic cod in the Northwest Atlantic (Swain, 1993) and scavenging, deep-sea fishes in the Northeast Atlantic (Collins *et al.*, 2005). If larger individuals of a species somehow can compensate for the disadvantages of occupying deeper waters (less light, less food etc.) there might be benefits associated with it like reduced competition and lower temperatures. Temperature has a large influence on the distribution of virtually all fish species as most are ectothermic and metabolic rates are heavily influence by the ambient temperature (Clarke and Johnston, 1999). Laboratory experiments have suggested that larger cod caught in the Northwest Atlantic prefer cooler waters (Lafrance *et al.,* 2005). The larger individuals gain lower metabolic costs and prolonged lives from the deeper, cooler waters. Smaller individuals on the other hand are thought to prioritize higher temperature than their larger conspecifics because the they gain advantages through increased growth rates and often higher prey densities with warmer, shallower areas (Árnason, Björnsson and Steinarsson, 2009). This means that, if they survive, they spend less time in the size groups that experience the highest predation pressure. In 2018

an article was published suggesting that fisheries may be the driver for Heincke`s law and tested this hypothesis on Atlantic cod in the western Atlantic (Frank, 2018). Most of the species where ontogenetic deepening has been observed are commercially fished and since fishing focuses on the larger individuals, we are effectively removing the larger fish from certain areas, leaving the smaller ones. If the fishing pressure is reduced as depth increases, it could create a pattern of increasing average size with depth.

The lack of consensus and multitude of proposed explanations for Heincke´s law suggests that, depending on the species and geographic location, different factors govern this pattern. Or perhaps that we have been looking in the wrong place. What if some physiological aspect of fish changes as it grows, allowing larger individuals to take advantage of the reduced competition and temperatures they are expected to encounter at greater depths?

To this day, no one has looked at Heincke`s law through the lens of allometry; the scaling of organs with regards to the size of the animal, or if physiological changes to sensory organs like the eye can impact depth distribution. Visual predation is dependent on two major factors; the amount of light available and the organism's capability to utilize that light. Due to waters ability to absorb and scatter light, as depth in the ocean increases, light decreases exponentially. That means that a more sensitive eye would be required to be able to forage effectively for food at greater depths. Most fish are visual predators (Guthrie, 1986, p.75) and this seems to apply to Atlantic cod as well (Brawn, 1969; Kotrschal, Van Staaden and Huber, 1998). So, if eye size increases as Atlantic cod get larger, this could possibly compensate for the lower irradiance levels at greater depths. This might allow a larger cod to have the same visual range at a greater depth as a smaller conspecific closer to the surface. As visual range influences encounter rates and feeding rates (Aksnes and Utne, 1993; Aksnes and Giske, 1997) the size of the eye should influence what depths cod can forage successfully. However, since the energy requirements increase with size as well, the larger cod would have to overcompensate and actually increase its visual range with depth compared to a smaller cod occupying shallower waters.

The aims of this study are threefold. 1) I will investigate whether Heincke´s law applies to the NEAC by analyzing survey data. 2) Parameterize a model to investigate how visual range and prey encounter rate changes with cod size and depth. Finally, 3) I will determine whether increased prey encounter rates as a consequence of increased visual range in larger cod can compensate for the increased energy needs associated with larger sizes.

2. Materials and Methods

2.1.1 Northeast Arctic Cod

The Altantic cod stock in the Barents Sea is called Northeast Arctic cod (NEAC) and will be the focus of this thesis. The NEAC is the migratory stock and having spent their juvenile stage in the Barents Sea, mature individuals undertake long, seasonal migrations to warmer spawning grounds along the Norwegian coast (Ottersen, Michalsen and Nakken, 1998). The most important spawning grounds are found around Lofoten and Troms, but some fish migrate as far south as Sotra (60°N) to spawn (Yaragina, Aglen and Sokolov, 2011). The age of maturation ranges from 6-9 years old (Ottersen *et al.*, 2014). For the time spent in the Barents Sea, the NEAC is widely distributed from Svalbard and the Great Bank (80°N and 78°N respectively) to the western part of Novaya Semlya and the Norwegian coastline in the south. The NEAC is highly adapted to the shifting conditions of the Barents Sea and can be found at temperatures between 0-7ºC, although they seem to avoid temperatures below 1-2ºC in winter (Jakobsen and Ozhigin, 2011, p. 227.) They mainly occupy depths between 100-300 meters, though individuals have been found as deep as 600 meters.

The NEAC is a major piscivore in in the Barents Sea (Hamre, 1994). Diet changes with age, shifting from mostly krill and amphipods for 0-, 1- and 2-year-old NEAC to mostly fish for older individuals (Dalpadado and Bogstad, 2004). Local prey availability does influence diet and though individuals 2 years and older mostly feed on fish (capelin and herring) they will consume shrimp, krill and squid among other organisms (Johannesen, *et al.*, 2012). However, capelin (*Mallotus villosus*) is considered the most important prey items for NEAC (Dolgov, 2002; Johannesen, Johansen and Kursbrekke, 2015) and the biomass production of capelin is one of the most important factors influencing the obtainable yield of the stock (Hamre, 2003). For this reason, capelin has been used as the prey item in my model.

2.1.2 The Barents Sea

The Barents Sea is a shallow, continental shelf sea with an average depth of about 230 m that covers an area of about 1.4 million km^2 (Smedsrud *et al.*, 2013). It lies in between the Northern coast of Norway and parts of Russia in the south, the archipelagoes of Svalbard and Franz Josef Land in the Northwest-and-east, respectively and Novaya Semlya in the East. The topography of the sea bed is characterized by several shallow banks with deeper areas in between (Figure 1.) The Central Bank, the Grand Bank, Tromsøflaket, Svaldbard Bank, Hopen and areas around Bjørnøya are all highly productive and extensively used by commercial fisheries (Olsen *et al.*, 2009).

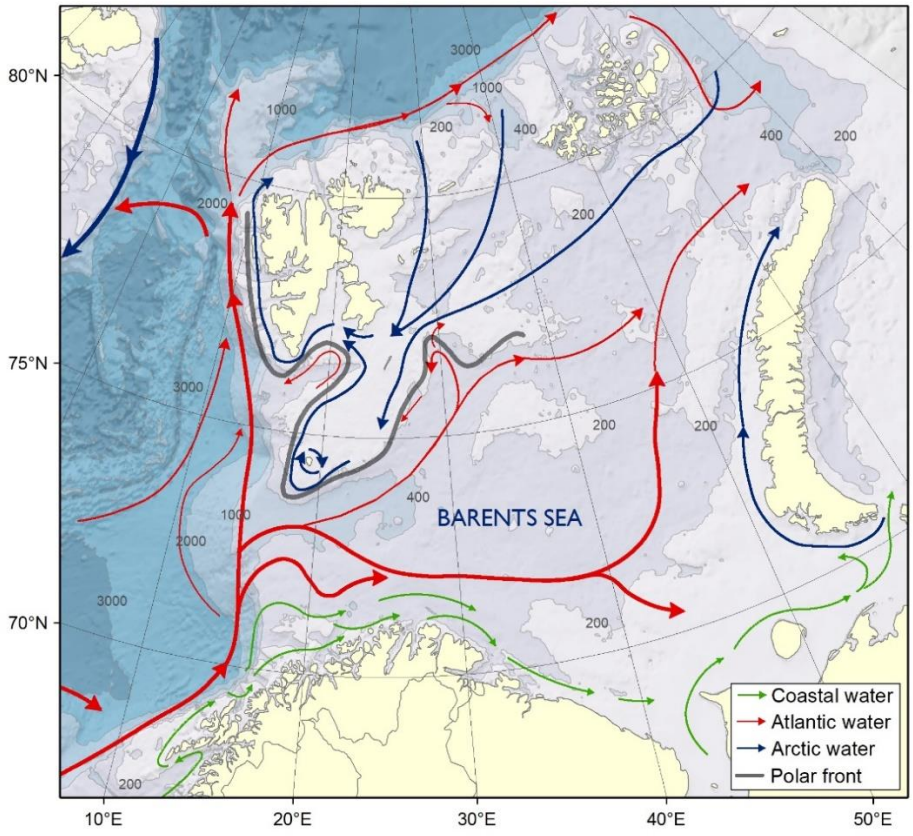

Figure 1. The main currents and bathymetry of the Barents Sea. Map created by Gjertsen and Ingvaldsen / IMR.

Three water masses are responsible for the physical conditions in this ocean; the Atlantic water, the Arctic water and the Coastal water, which in turn are connected to three currents

(Loeng, 1991). The shallow depth is partially responsible for the productivity of the sea. Warm Atlantic water gets pushed up by the continental shelf edge that runs from just North of Lofoten to the western part of Svalbard. This inflow of water helps keep the sea partly ice free during the winter. In the Barents Sea, the Atlantic water mixes with the cold Arctic water. This mixing causes upwellings that draw nutrients towards the surface where phytoplankton can utilize it. This leads to high levels of primary production (except during the winter months.) This, combined with a large area and sustainable management, allows the Barents Sea to support the largest stocks of cod and haddock in the world.

2.2.1 Empirical Data Collection

To investigate whether or not the NEAC showed evidence of a bigger-deeper pattern, I analyzed data collected from the joint Norwegian-Russian ecosystem surveys (BESS) that started in 2003 and are run annually from August-October in the Barents Sea. The Institute of Marine Research (IMR) is the Norwegian partner and Polar Research Institute of Marine Fisheries and Oceanography (PINRO) is the Russian partner. Between four and five ships are used, three Norwegian vessels and one or two Russian ones. (https://www.imr.no/tokt/okosystemtokt_i_barentshavet/toktrapporter/nb-no.) The number of trawl stations for each year can be found in Table 1. Only data from the Norwegian vessels were used, to make sure that sampling technique and estimated catch per distance remained the same between all stations and all years. The number of stations for each year is, in part, affected by how the vessels have been distributed across the Barents Sea and how many Russian vessels that were attending the survey. The sampling techniques and equipment are described under 'Sampling Manual' on IMR´s webpage for BESS (https://www.imr.no/tokt/okosystemtokt_i_barentshavet/sampling_manual/nb-no.) Any deviations from the Sampling Manual can be found in 'Technical Report'. Catch was weighted against trawling distance so that all data represents catch per nautical mile. The catch was brought down to the on-board laboratory where it was weighed, length measured to the nearest centimeter, and gender was determined. Data regarding depth and position of capture (station), year, month and which vessel that was used were collected and stored on the on-board servers. Bottom depth was measured for each station with the use of the on-board echo sounder.

Tabel 1. This table shows the number of trawl stations during the BESS for each year. Note that only trawls done by Norwegian vessels have been counted and used in this thesis.

Year	Nr. of stations	Year	Nr. of stations	Year	Nr. of stations
2003	201	2008	654	2013	746
2004	785	2009	336	2014	277
2005	909	2010	300	2015	303
2006	850	2011	366	2016	255
2007	771	2012	397	**SUM:**	**7150**

2.2.2 Testing for Heinckes Law With Empirical Survey Data

I took the data regarding year, depth and size-range for 2003-2016 and combined it into one Excel document, comprised of 7150 rows, where each row represents a station. I only utilized depths <500 m as cod are not regularly found deeper than this and very few areas of the Barents Sea are this deep. I pooled the data into 10 cm length groups. Length-groups ranged from 25-34 cm to 115-124 cm. I disregarded fish <25 cm, as they were caught poorly by the trawl and would therefore not be giving a presentable depth distribution. The fish >125 cm was also excluded as few individuals this large were caught. I then used R studio to study the mean depth with regards to length groups, for regression analyses and plotting of the data. The script used for all analyses and graphs can be found in Appendix 3. To calculate the weighted mean depth of the different length groups I used the following equation;

$$1.\ D_j = \frac{\sum_{s=i}^{n} D_s N_{j,s}}{\sum_{s=j}^{n} N_{j,s}}$$

where D_j is the average depth of length group j, D_s is the bottom depth at station s, $N_{j,s}$ is the number of cod caught in length group j at station s, and n is the number of stations. This

calculation was done using R. The average depth for each length-group was plotted using a scatterplot and a linear trend line was added. A linear regression analysis was conducted to investigate whether mean depth changed significantly with size.

A probability density function (PDF) for each length group was calculated and plotted with a smoothing function (Gaussian Kernel, default for R). The PDF allowed me to investigate how the distribution of the cod compared to the different depths sampled, thus revealing how their depth preferences might change. A line chart was made for each length-group showing their probability density distribution where the area under the line always equaled one. A second line was added that showed the depths sampled and the area underneath it was colored grey. These charts where then combined to a single figure.

A cumulative frequency distribution was also estimated to investigate over which depths most of the catch was made. To do this, the following equation was used;

$$2.\ Share\ C_{d,N} = \frac{\sum_{n=d_0}^{d} C_{d,N}}{\sum_{n=d_0}^{dn} C_N} \times 100$$

where *Share* $C_{d,N}$ is the percentage of the total catch caught before depth *d* for length group *N*, $C_{d,N}$ is the cumulative catch at depth *d* for length group *N*, d_0 is the shallowest depth sampled, d_n is the deepest depth sampled and C_N is the total catch of length group *N*.

2.3.1 Encounter Rates as a Function of Visual Range

Encounter rates influences the energy intake of any predator. As the number of prey items a predator can encounter increases, so does the probability of it satisfying its required daily energy intake. In an aquatic environment, this encounter rate is strongly dependent on the visual range of the predator. Visual range is in turn governed by several factors, such as light levels, eye sensitivity, prey size and contrast.

To estimate prey encounter rates, I used a simple geometric based encounter rate equation, similar to the one used in Aksnes & Giske (1993.) The equation:

$$3.\ E = \pi(r\ sin\theta)^2 vN$$

estimates the prey encounter rate (E) of a given fish, depending on visual range (r), visual half angle (θ), swimming speed (v) and prey abundance (N). Swimming speed is usually measured in body lengths s^{-1} (BL s^{-1}). A study from 1993 showed that the average cruising speed for a juvenile cod was 0.6 BL s^{-1} when food intake was half of the maximum intake rate (Björnsson, 1993). I chose this value because I assumed it would be representative value for the average velocity cod would travel at in the wild. The visual half angle used was θ=30° (Lueck and O´Brien, 1981; Dunbrack and Dill, 1984) as this was used by Aksnes and Giske (1993). The value for prey abundance was acquired from Johanna Fall (pers.com.). This value was derived from an estimated number of capelins per strata over a certain depth (100 m), based on actual values from the ecosystem surveys that IMR run yearly. The value changed depending on which areas were considered, but a conservative estimate was 0.0004 capelin m^{-3} for the entire Barents Sea. Hence, I chose to operate with this value. In essence, Eq. 2 is just a measure of the volume of water a fish can search through in a given time, with the prey abundance per volume of water added. A visual representation of how the different parameters produce the encounter rate can be seen in Figure 2.

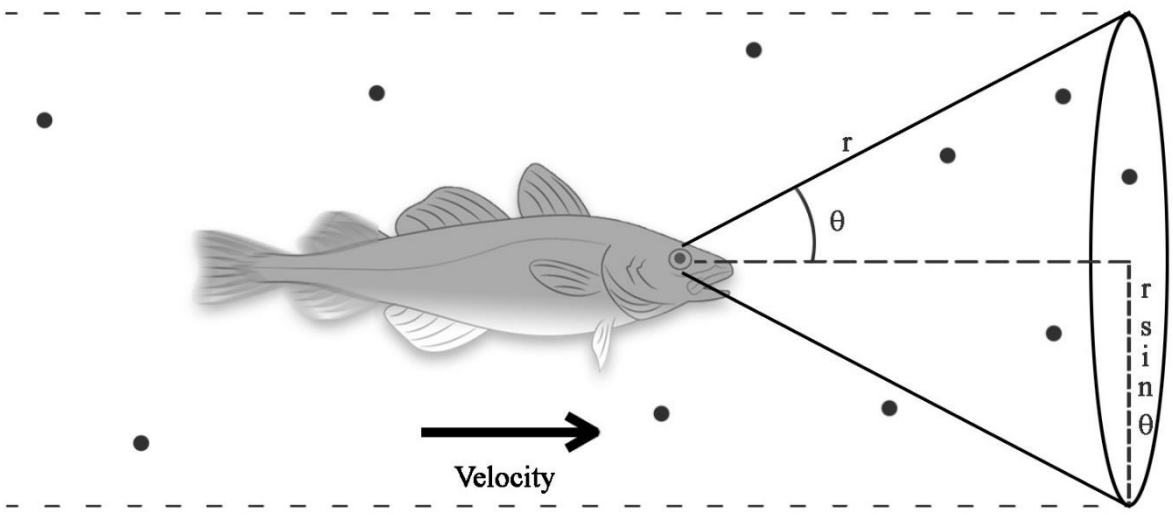

Figure 2. A visualization of the different parameters influencing encounter rate. Velocity will vary with cod size and visual range with cod size, depth, prey size and contrast. The figure is a modified version of the one found in Aksnes and Giske (1993.)

To be able to properly predict encounter rates for different sized cod found at different depths, I had to calculate their visual range. All visual range models need to take into account that there are certain physical and biological limitations that govern the world of vision (Barten, 1992; Greivenkamp *et al.*, 1995;). First off, light levels are important. This is true for animals in any environment, but water scatters, refracts and absorbs light to a much greater extent than air (Lythgoe, 1988, Ch. 3) and as depth increases, light levels decrease exponentially. This means that below a certain depth, not enough photons reach the photoreceptors on the retina to produce a neurological response; the irradiance threshold. The maximum depth would vary depending on the species of fish, as these have evolved to cope with the light levels of their environment, but all visual predators in an aquatic environment would at some point reach a minimum irradiance threshold.

Next, the projection of the prey on the retina has to be large enough to produce an image. The size of this image is dependent on two things; the actual size of the prey and the distance between the fish and the prey. If the prey is too small, it will not produce a large enough image on the retina to enable detection. If the distance between the prey and predator is to great, the area of the prey on the retina also becomes too small for detection. What minimum

size and maximum distance is depends on the sensitivity of the retina and mosaic of photoreceptors which in turn depends on the species of fish and perhaps the size and/or age.

To be able to detect a prey item requires a threshold difference in the flux of light at the retina in the areas with and without the prey image. This would depend on the sensitivity of the retina, but also the contrast between the prey and background. A pale prey would stand out against a dark background (like the surrounding water) but would be harder to distinguish against a light background (like the water surface.) The opposite would be true for a dark prey. The threshold difference in flux of light at the retina would vary with predator species, while the contrast is a trait of the prey.

These factors are the basis for any visual range model. Other aspects like the size of the eye and beam attenuation coefficient of the water will influence how much light that reaches the retina and in that way affect visual range. As beam attenuation is a property of the water, eye size is the only factor influenced by the size of the fish and under evolutionary pressure.

2.3.2 The Basis for My Visual Range Model

I modified an existing model from Aksnes & Utne (1997) so that it would take into account how the change in lens size affects visual range. A detailed explanation of the assumptions of the model, along with choice of parameters and variables can be found in Aksnes & Giske (1993) and Aksnes & Utne (1997). The original model was the following:

$$4.\ \ r^2\, exp(cr) = |C_0| A_p \frac{E_b}{K_e + E_b} E_{max}\, \Delta S_e^{-1}$$

where r is the visual range, c is the beam attenuation coefficient of the water between the prey and the eye, C_0 is the prey´s inherent contrast, A_p is the area of the prey and ΔS_e is a sensitivity parameter that is species specific. As contrast (C_0) can be viewed as both a positive (white on dark background) and negative (dark on white background) value (Thetmeyer and Kils, 1995), the absolute value was used.

I rewrote Eq. 4 to allow for iterative solving and Equation 5:

$$5.\ r = \sqrt{\exp(-cr)|C_0|A_p \frac{E_b}{K_e+E_b} E_{max}\ \Delta S_e^{-1}}$$

was used in combination with Excel´s iterative option to produce visual ranges for cod´s of different sizes and at different depths.

2.3.3 Lens Size

Now that I had my basic equation for calculating visual range, I needed a way to incorporate increased lens size into it. A summary of the optical structure of fish can be found in Appendix 2. In its original form, Equation 4 did not explicitly utilize eye size as a parameter. However, the ΔS_e parameter is composed of several other parameters, including the focal ratio of the fish eye. The focal ratio (focal length/lens radius) of the average fish eye was first established by Ludwig Matthiessen in the early 1880´s (Matthiessen, 1882). He calculated, from a series of measurements of fish eyes, that there existed a fixed ratio between focal length and lens radius for fish. This number, known as Matthiessen`s ratio, turned out to be 2,55 times the radius of the lens, regardless of fish size. J. D. Sadler (1973) showed, through laboratory experiments, that an average estimate of the focal ratio of a cod is 2,56 times the radius of the lens. Since focal length is the product of the lens radius and focal ratio, this gave me a way of calculating visual range based on eye size. Thus, Sadler´s discovery could be represented by the following equation:

$$6.\ f = 2{,}56 \cdot r_{lens}$$

where f is the focal length and r_{lens} is the radius of the lens (in mm.)

2.3.4 Modelling Light Processing in the Fish Eye from Radiance to Neural Signal

Aksnes & Giske (1993) stated that the sensitivity of the eye (ΔSe) is the ratio between the sensitivity of the retina (ΔS_r) and the focal length (f) and light absorption of the lens (k). Equation 7 is presented here:

$$7.\ \Delta S_e = \Delta S_r / k f^2$$

where the k-value represents the amount of light that passes through the lens and surrounding eye fluid and reaches the retina, ΔS_r represents the eye-specific sensitivity and ΔS_e represents the sensitivity threshold for recognizing the prey according to retinal flux. The k-value was taken from Aksnes & Giske (1993) and is based on the fact that only 10% of the light that passes through the eye reaches the retina in humans (Sternheim and Kane, 1986, p. 599.) Being a visual predator in a marine environment, it is not unrealistic that fish could have developed clearer lenses and eye fluids than mammals as to make the most of the light available. However, as I found no studies done on the clarity of a fish lens providing me with a different value, I chose to use the one from Sternheim and Kane.

The ΔS_r and ΔS_e parameters represent the sensitivity of the eye as a whole. Put simply, ΔS_r is the light sensitivity measured at the retina while ΔS_e is the light sensitivity measured at the cornea. To be able to calculate ΔS_e, I first needed to establish ΔS_r. Meager *et al.* (2010) did a series of experiments on reaction distance with juvenile cod under different light intensities. They also compared their findings with the theoretical model from Aksnes & Utne (1997) and parameterized it to be within 5% of their measurements. For the model to fit with their experimental data they had to introduce two different values for the visual capacity parameter $E_{max}\,\Delta S_e^{-1}$ depending on the light levels (for light intensities <5 μmol m^{-2} s^{-1}, $E_{max}\,\Delta S_e^{-1}$=11000 gave the search lengths most congruent with the experimental data; for light intensities >5 μmol m^{-2} s^{-1}, $E_{max}\,\Delta S_e^{-1}$=25000 was more appropriate.) As light levels at depths most relevant for my thesis (>150 m) were <5 μmol m^{-2} s^{-1} given the surface irradiance values and the vertical attenuation coefficients I used, I chose to operate with $E_{max}*\Delta S_e^{-1}$=11000. To simplify matters, I assumed E_{max}=1 μmol m^{-2} s^{-1}. This allowed me to calculate ΔS_r by substituting ΔS_e in the $E_{max}*\Delta S_e^{-1}$ parameter with equation 4. The value for ΔS_r then became $3.7*10^{-10}$ μmol

m^{-2} s^{-1} for a given *f*-value and I have assumed that this value is constant for all sizes. This would then allow me to use Eq. 4 to estimate how ΔS_e changed as lens radius increased.

The K_e-value was introduced in Aksnes and Utne (1997) along with E_{max} to account for non-linear transformations of light energy into neural responses. Changes in the retinal response, like going from photopic (cone based) to scotopic (rod based) vision or other, unknown neural responses, could give non-linear changes in the visual range. These changes needed to be accounted for if the model was to accurately predict a cod´s visual range. As stated in Aksnes and Utne (1997) the K_e-value (and E_{max}-value) could be estimated if the visual range was established through controlled experiments. Meager *et al.* (2010) calculated that K_e=0.0001 μmol m^{-2} s^{-1} for light intensities <5 μmol m^{-2} s^{-1} was appropriate. Given the depths, surface irradiance and turbidity levels I´ve operated with, K_e=0.0001 μmol m^{-2} s^{-1} was appropriate, as I was dealing with light levels are below 5 μmol m^{-2} s^{-1}.

From Equation 5 and 6 it became apparent how the sensitivity threshold of the fish eye parameter (ΔS_e) was directly linked to the size of the lens. This allowed me to implement lens size into equation 4 and calculate a visual range given different eye sizes. As lens size would increase, ΔS_e would decrease.

2.3.5 Modelling Light in Water; Irradiance, Vertical Attenuation Coefficient and Beam Attenuation Coefficient

The light levels at depth depend on the light levels at the surface, the depth and the clarity of the water. When passing through a medium of thickness *z*, light levels decay in accordance with Beer`s law (Beer, 1852) and for water, light levels at depth can be calculated by using the following equation;

$$8.\quad E_b(z) = pE_0\exp(-Kz)$$

were E_0 represented the light intensity above the surface, *p* is the amount of light lost in the air-sea interface, *K* is the vertical attenuation coefficient and *z* is the depth. The light intensity variable (E_0) changes radically depending on time of day, cloud cover and season, ranging

from 1800 μmol m^{-2} s^{-1} (cloudless day in summer) down to 100 μmol m^{-2} s^{-1} and below (Sakshaug and Slagstad, 1991). Irradiance measurements from parts of the BESS gave a daily average irradiance of 59 μmol m^{-2} s^{-1} over three days (Johannesen, pers. com.) Several different values for *p* can be found depending on where you look. Aksnes & Giske (1993) operated with *p*=0.5 whilst an article on solar irradiance in maritime atmospheres (Gregg and Carder, 1990) concluded that for most weather conditions, the p-value should be between 0.84-0.95. Since the *p*-value seemed so variable, I used 59 μmol m^{-2} s^{-1} as a combined pE_0-value.

The amount of light at depth is not just dependent on surface irradiance, it is also influenced by the turbidity of the water, also known as the *K*-value. The *K*-value varies with location and time of year. Open ocean water can have a K-value as low as 0.06 m^{-1} (Skaret *et al*., 2016, p. 14) after the plankton blooms have subsided (fall/winter.) In contrast it might be >0.2 m^{-1} closer to the coast during the algal blooms in summer (Øyvind Fiksen, pers. com.) For the calculations of how visual range changed in accordance with size and depth, *K*=0.08 m^{-1} was used, as this was the mean attenuation coefficient measured during one of the ecosystem surveys of the Barents Sea during autumn (Aarflot *et al.*, 2018.) The beam attenuation coefficient (*c*) was calculated based of *K*. *c* is dependent on *K* (Phillips and Kirk, 1984, as cited in Aksnes and Giske, 1993) and in clear water *c* is usually was 2-4 times higher than *K*. I therefore chose to use *c*=3*K* for all calculations. Depth would then be the only variable and I could investigate the effect it had on visual range for the different length groups of NEAC.

The light-at-depth equation (Eq. 8) was used for two different calculations. First, I used it to estimate the environmental background irradiance at 195 m, as this was the median depth for all the length groups investigated in this thesis, and get an estimate for how visual range would change depending on cod size. Then, I used Eq. 8 to calculate the irradiance levels at the average depths for each length groups (estimated from the data from the BESS) so I could investigate how visual range and encounter rates would change as the larger fish went deeper. All visual range calculations used a pE_0=59 μmol m^{-2} s^{-1} -, *K*=0.08 m^{-1} and *c*=0.24 m^{-1}.

2.3.6 Prey Size and Contrast

As mentioned earlier, the size and contrast of the prey item will influence the cod´s visual range. As I´ve assumed that the prey item is capelin, the size of the prey was based on this species. Mature capelin range in size from around 13 cm to 20 cm for adult males (Luna and Valdestamon, 2018). For my estimates of visual range, I used a length of 10 cm, as this is a size where most capelin has metamorphosized into the mature form (Gjøsæter, 1998) and I assumed this length could be eaten by all the length groups of cod I have been working with. The equation used for calculating prey area was based on the equation for calculating the area of an ellipsis ($A= \pi*a*b$). *a* would represent the body length of the prey and *b* would represent the body depth. The average body depth for capelin in the North Atlantic has been found to be ~18% of the body length (Schultz, 1937). Since *b* is dependent on *a*, the calculation became $A=\pi*a^2*0.18$. Area was calculated as m^2.

I took the contrast (C_0-value) from an experiment on the visibility of herring and mysids in the Baltic Sea (Thetmeyer and Kils, 1995), which was Meager *et al.´*s source as well. I chose to use this paper as a reference, as both herring and capelin share similar, silvery flanks. Thetmeyer & Kils reported contrast values ranging from roughly 0.1 and 0.7. Though Meager operated with C_0=0.3 for a mysid (*Praunus neglectus*), which is slightly transparent, I was unable to find any information on the contrast levels of capelin. Hence, I have assumed C_0=0.3 when I calculated how fish size influenced visual range. This parameter is dimensionless as it represents the portion of light reflected of the prey.

2.3.7 Solving for *r*

All the parameters used for calculating how visual range changed with cod size are represented in Table 2. Because of the nature of the model, some iteration was necessary to balance the equation and figure out what the visual range (*r*) value had to be. Using Excel´s iteration option, I was able to calculate *r*-values that would balance Equation 5. The left side of the equation (*r*-value) was placed in one cell, while the right side was placed next to it. I then enabled Excel´s iteration option and set the *r*-value cell to equal the neighboring cell. 10 000 iterations were used with a maximum change of 0.01 per iteration to give an *r*-value that would make the cells equal each other. The change in visual range on the right side of Eq.

4 came from the ΔS_e parameter, which was linked to the lens size through Eq. 5 and 6. This iteration technique was used for investigating the effect of depth as well.

I used the median size of each length group (30 cm for length group 25-34, 40 cm for length group 35-44 etc.) to calculate the visual range for length groups at their average depth. Light levels at depth was calculated based on Equation 8 with a surface irradiance of 59 μmol m^{-2} s^{-1} and K=0.08 m^{-1}.

Table 2. Parameters used for calculating visual range for different sized cod using Equation 3. The source shows the article the value was taken from. If nothing is stated, the value has been calculated or estimated.

Symbol	Explanation	Parameter	Unit	Source
A_p	Prey area	~0.0057	m^2	-
c	Beam attenuation coefficient	0.24	m^{-1}	Phillips and Kirk, 1984
C_0	Prey contrast	0.3	dimensio n-less	Thetmeyer & Kils, 1995
E_0	Surface irradiance	59	µmol photons m^{-2} s^{-1}	CODFUN 2016114 Barents Sea Survey
E_{max}	Maximal retinal irradiance that can be processed	1	µmol photons m^{-2} s^{-1}	Assumed
K	Vertical attenuation coefficient for irradiance	0.08	m^{-1}	Aarflot *et al.*, 2018
k	Ratio between radiance at retina and lens	0.1	dimensio n-less	Sternheim & Kane, 1986
K_e	Composite saturation parameter reflecting adaptational processes and light/neural transformation	0.0001	µmol photons m^{-2} s^{-1}	Meager *et al.*, 2010
ΔS_r	Sensitivity threshold for detection of radiant flux on retina	$3.7*10^{-10}$	µmol photons s^{-1}	Estimated from Meager *et al.*, 2010

To be able to examine the effect increased lens radius had on visual range and whether it could compensate for the reduced light levels at increasing depths, I had to investigate if lens size increased with body size. To do this, I procured cod heads from a local fish shop (Jensvoll Fisk). I acquired a total of 21 cod heads that came from Lofoten and the Barents Sea area. First, I measured the head lengths (dorsally) from the tip of the snout to the end of the head to the nearest 0.5 cm using a tape measure. I removed the eye and opened it to remove the lens by making an incision into the side of the eye with a scalpel, carefully, as not to damage the lens. The lens diameter was measured down to the nearest 0.5 millimeter using a plastic caliper (8 cm long, Clas Ohlson.) I then investigated if lens radius increased with body length. Kjell Nedraas at IMR (pers. com.) had done some work on the relationship between total cod length (cm) and head length (cm) and I was able to use an equation he had formulated to translate my measured cod head lengths into total body lengths. The relationship is expressed by the following regression model:

$$9.\ L = 4 + 3.65H$$

that applied to cod caught North of 62° which was the case for the specimens I had. *H* is the length of the head (cm) while *L* is the predicted body length (cm). Standard deviation for this prediction was 4.1 cm according to Nedraas work. Utilizing this equation, I was able to predict an estimated length for the cod heads I possessed.

I used the measured lens radii and estimated body lengths (from head size) to estimate how lens size increases as the cod grows larger. In total, 23 lens radii were plotted against body length, including 2 values from Sadler (1973). Sadler used cod lenses to investigate the focal ratio of this species and used cod ranging from 27 cm to 52 cm. His largest and smallest lens radius was 2.9 and 4.4 mm. I assumed that these lenses belonged to the smallest and largest cod respectively. These data were plotted against each other to investigate the relationship (Figure 3.)

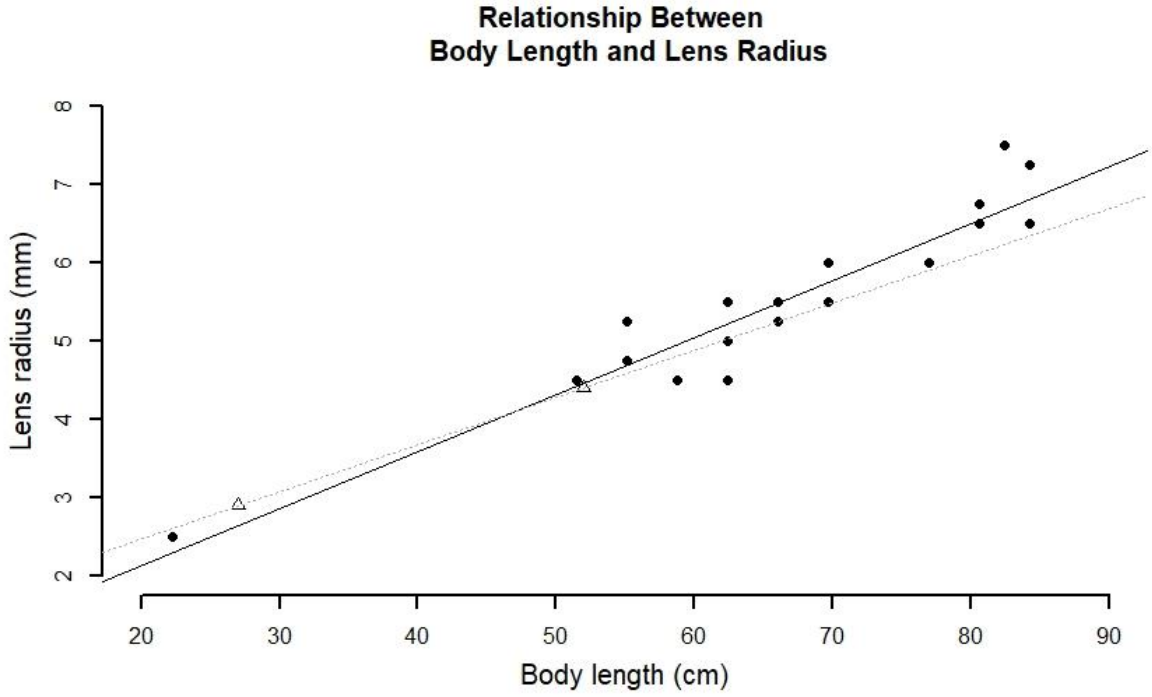

Figure 3. The relationship between the lens radii and cod lengths. The triangular points are taken from another article (Sadler, 1973) whilst the circular ones are measured by me (for these, cod length is estimated based on Equation 7.) The solid, black trendline is for my data, while the dotted, grey trendline is for Sadler´s data.

A linear trendline was fitted (adjusted R^2=0.886) and an equation for the trendline was estimated. The trendline equation was the following:

$$10.r = 0.67273 + 0.07275L$$

where *r* is lens radius (mm) and *L* is total body length (cm). Eq. 10 would then be used to establish lens sizes for cod over a range of body lengths (25 cm to 124 cm, in 1 cm increments.)

2.4 Effect of Body Size on Encounter Rate and Energy Requirements

To investigate the last aim of this thesis, I needed to examine how energy requirements, visual range, encounter rates changed with body size. Energy requirements are dependent on size, basal metabolism, activity levels, growth and reproduction. I focused on basal metabolic rate, also known as standard metabolic rate (SMR.) This was done to simplify the work, as growth rates, activity levels and reproductive output changes with age and time of day and/or year and would therefore introduce an unnecessary level of complexity in an attempt to answer the questions of this thesis. As SMR is influenced by volume more than length, I needed to establish the weight of the length groups I worked with. Using length and weight data from cod caught in the Barents Sea between 2004 and 2015, I produce a length-weight relationship plot (Figure 4) in R, while Excel was used to produce an equation for this relationship.

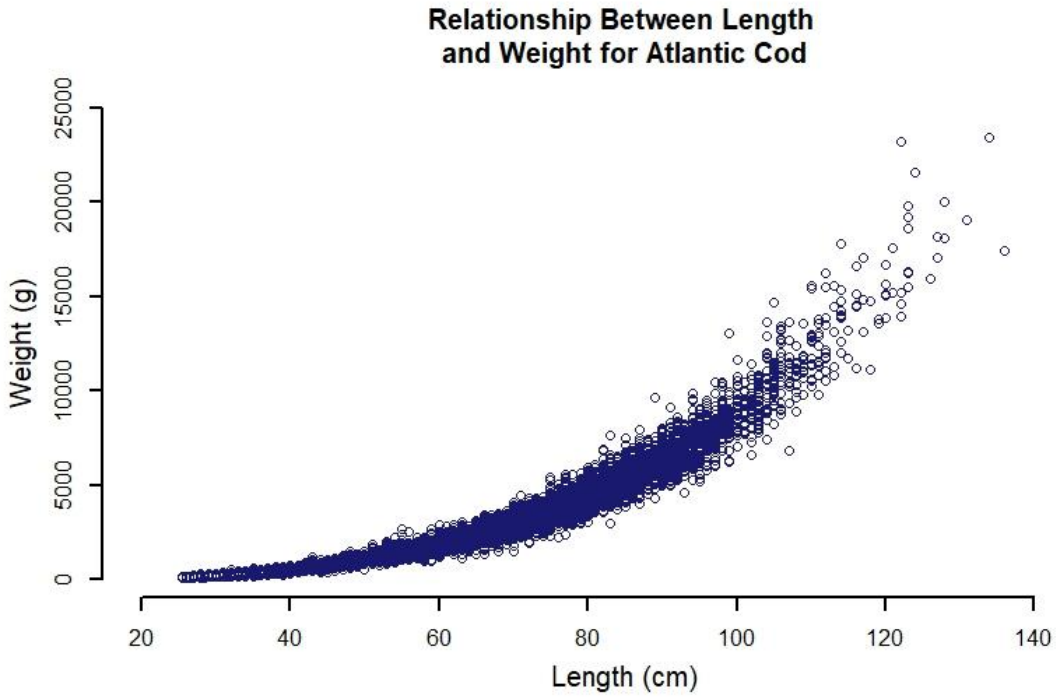

Figure 4. The plot used to obtain equation 10. Weight has been plotted against length. The data was collected during the 2004-2015 IMR research cruises in the Barents Sea.

A power function was the closest fit (R^2=0.9881) and provided the following equation:

$$11. W = 0.0076L^{3.0285}$$

where *W* is mass (in grams wet weight) and *L* is length (in cm). Eq. 11 would allow me to convert the lengths that I had calculated from Eq. 9 into wet weight, which in turn would allow me to estimate the energy requirements for a cod of a given size.

This allowed me to estimate the energy requirements for NEAC of different lengths. I used an equation for monthly SMR (Jørgensen and Fiksen, 2006) and transformed it to better fit with my temperatures and time frames. Firstly, Jørgensen and Fiksen operated with Joules per month (J $month^{-1}$) while I wanted kiloJoules per day (kJ day^{-1}) so that I could present the minimum daily energy required for an individual cod of a given size. This was done by simply converingt from month into days (I assumed 30 days $month^{-1}$) and Joules into kiloJoules (1000 J kJ^{-1}.) Secondly, they operated with a water temperature of 5°C while the BESS data suggested that the NEAC occupy water of between 1°C and 2°C during the time of the survey (Appendix, Figure A1.) Temperature influences the rate of biological processes (Prosser and Brown, 1961) and so a decrease in ambient temperature should result in a lower SMR. Thus, I needed to adjust the equation, so it fit my temperature range by using a Q_{10} factor of 2.06 (Karamushko, 2001) so I could get an SMR at 2°C. The equation then looked like this;

$$12. SMR = 0.071W^{0.828}$$

where W is the mass of the fish (wet weight in grams.) Eq. 12 would then give me an estimate of the daily energy needs (kJ day^{-1}) of cod of different sizes (Figure 5) and allow me to compare energy requirements to visual range and encounter rates as cod grew larger.

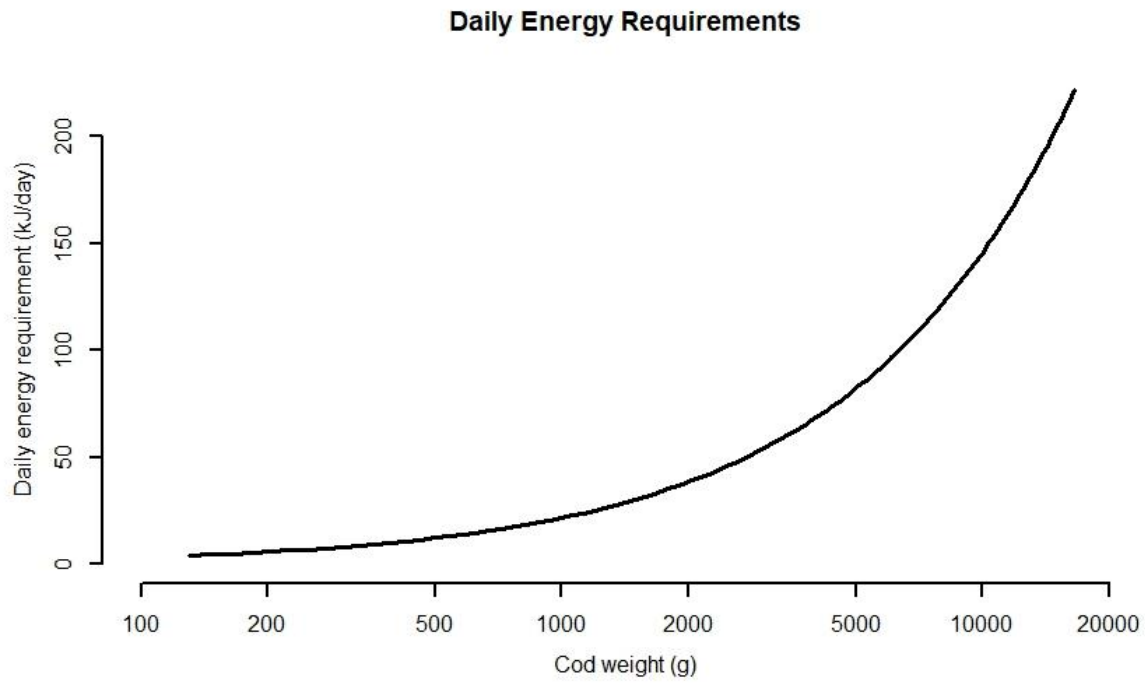

Figure 5. The daily energy requirements (SMR) for cod of increasing weight based on Eq. 12.

To establish the amount of energy that a cod of a given size theoretically could obtain based on encounter rates, I needed the energy density of the capelin. A 10 cm capelin would weigh approximately 5 g (Johannesen, pers. com.) and with an energy density of 8.95 kJ g^{-1}, that would constitute 40.25 kJ $capelin^{-1}$.

3. Results

3.1 Does Heincke´s Law Apply to The NEAC?

The probability density function (PDF show that the NEAC are distributed across almost all depths but show higher probabilities of being found at certain depths depending on size (Figure 6.) However, this pattern is more distinct in certain length groups compared to others.

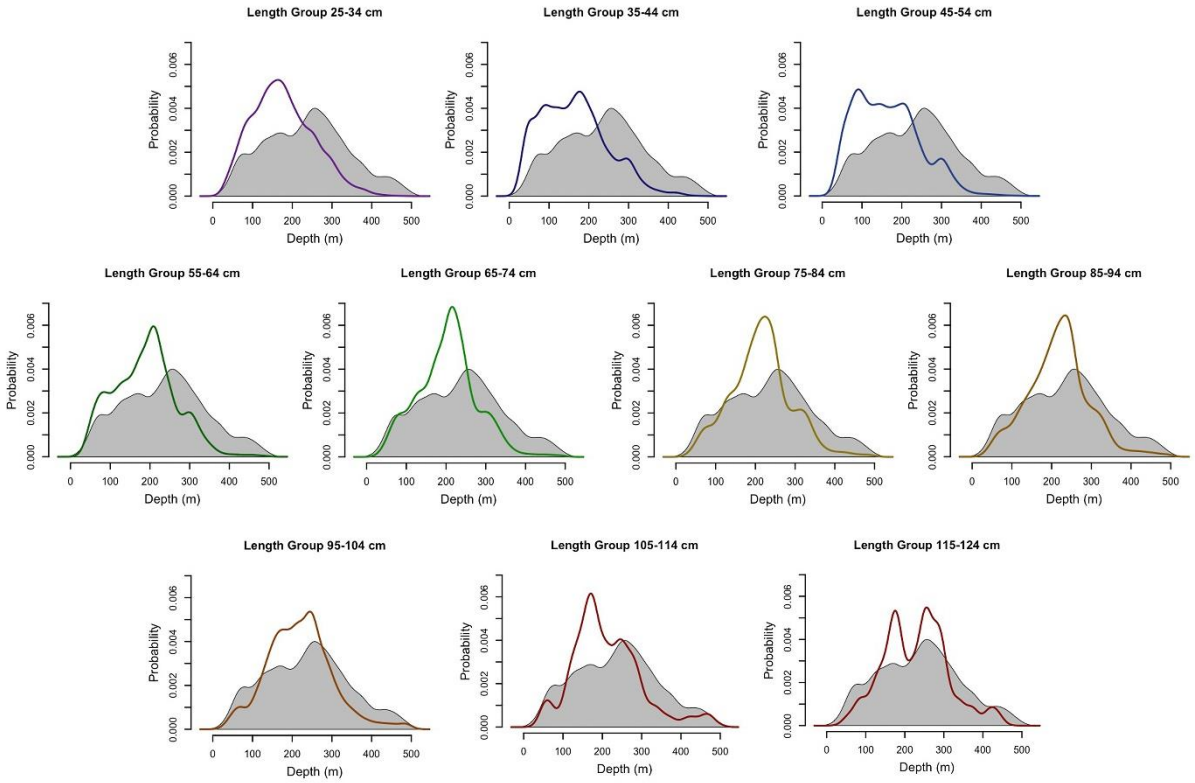

Figure 6. The PDF of cod of different length groups in the Barents Sea. The grey area represents the depths sampled and the proportion of samples taken at each depth.

Depths of approximately 300 m have been sampled more than any others. It can seem that the PDF of the larger length groups more closely follow the shaded area, representing available depths, than their smaller conspecifics. However, this has not been statistically analyzed.

The cumulative frequency distribution can be viewed in the Appendix (Figure A3.) This data was used to generate Table 3 and investigate at which depth range 50% of the total catch had been caught for each length group.

Table 3. The depths where 25% and 75% of the total catch group has been made for each length group.

Length group (cm)	Depth for 25 % of catch (m)	Depth for 75 % of catch (m)
25-34	121	228
35-44	93	212
45-54	97	212
55-64	129	235
65-74	157	243
75-84	168	251
85-94	168	255
95-104	162	266
105-114	160	262
115-124	169	285

On average, 50% of the total catch for all length groups have been caught over a range of 102.5 m (SD=12.4 m.)

While Figure 6 shows the depth distribution within each length group, Figure 7 presents the mean depth for each length group. A significant correlation between an increase in length and increase in mean depth is present (adjusted R^2=0.8014, $p<0.001$) indicating that larger NEAC occupy deeper waters than their smaller conspecifics.

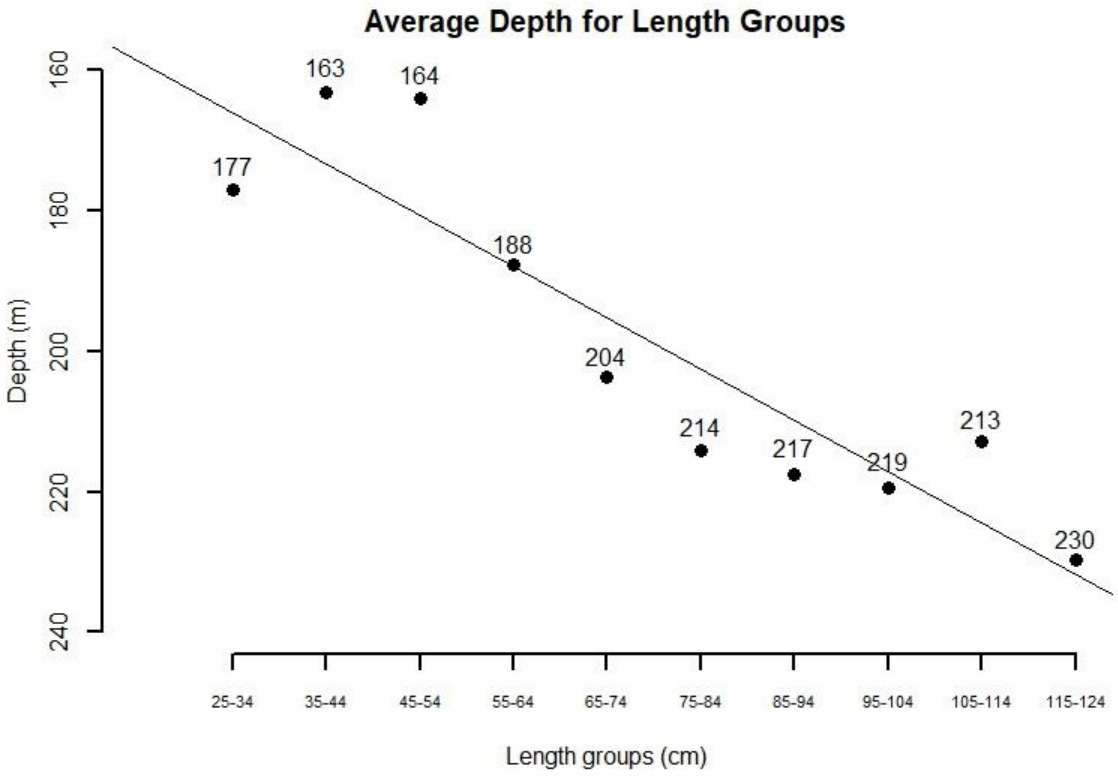

Figure 7. The average depth for different length groups plotted with a regression line. The number represent average depth rounded up/down to the closest integer. Because of the large sample size, standard error bars have been neglected, as these would have been hidden by the points in the plot.

The deepening pattern is mainly caused by the length groups between 45-54 cm and 85-94 cm, where the average deepening is 13.25 m per length group. Length groups outside this range contribute less to this pattern. The deepening per length group is 5.9 m when all length groups are considered.

3.2 How Does Increased Lens Size Affect Visual Range?

From Figure 4 (Materials and Methods) it becomes apparent that there is a significant correlation between the lens radius and total body length. This corresponds well with the data that Sadler (1973) had, although his article did not specifically look at this correlation. The effect the calculated lens sizes have on visual range is presented in Figure 8.

To get ambient light levels, I parametrized Eq. 7 to predict light levels at 195 m, as this was the mean depth for all the length groups.

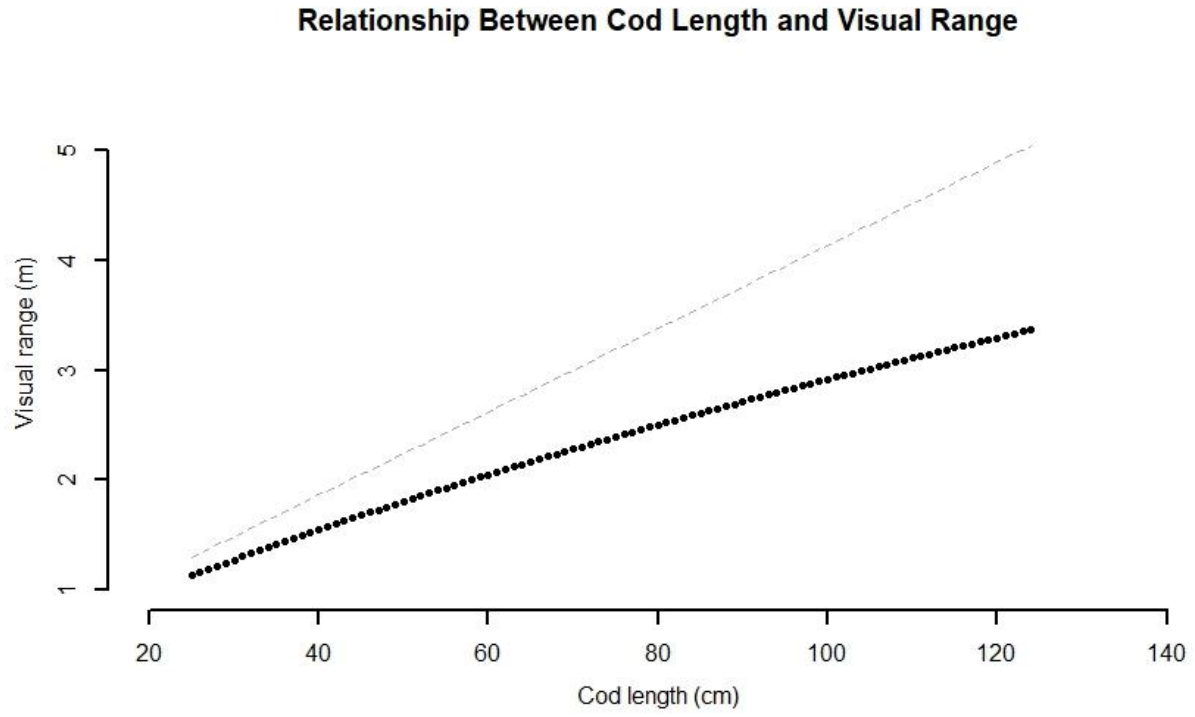

*Figure 8. The modeled visual range for different lengths using Eq. 8. All variables except ΔS_e were kept constant (c=0.24, A_p=5.65*10^{-3} m^2, C_0=0.3, E_b=9.90*10^{-6} µmol m^{-2} s^{-1}, K_e=0.0001µmol m^{-2} s^{-1} E_{max}=1 µmol m^{-2} s^1, k=0.1.) The dotted grey line show visual range without the beam attenuation coefficient (c=0) for comparison. Light levels at depth (E_b) was calculated using Eq. 7 (E_0=59 µmol m^{-2} s^{-1}, z=195 m and K=0.08 m^{-1}.)*

As length increases, so does visual range, but not linearly. This is due to the beam attenuation coefficient (*c*). As visual range increases, the amount of light that is scattered or absorbed, also increases, reducing the growth rate of the visual range. As the cod length increases, causing increased visual range (due to increased lens size), so does the effect of the beam attenuation coefficient.

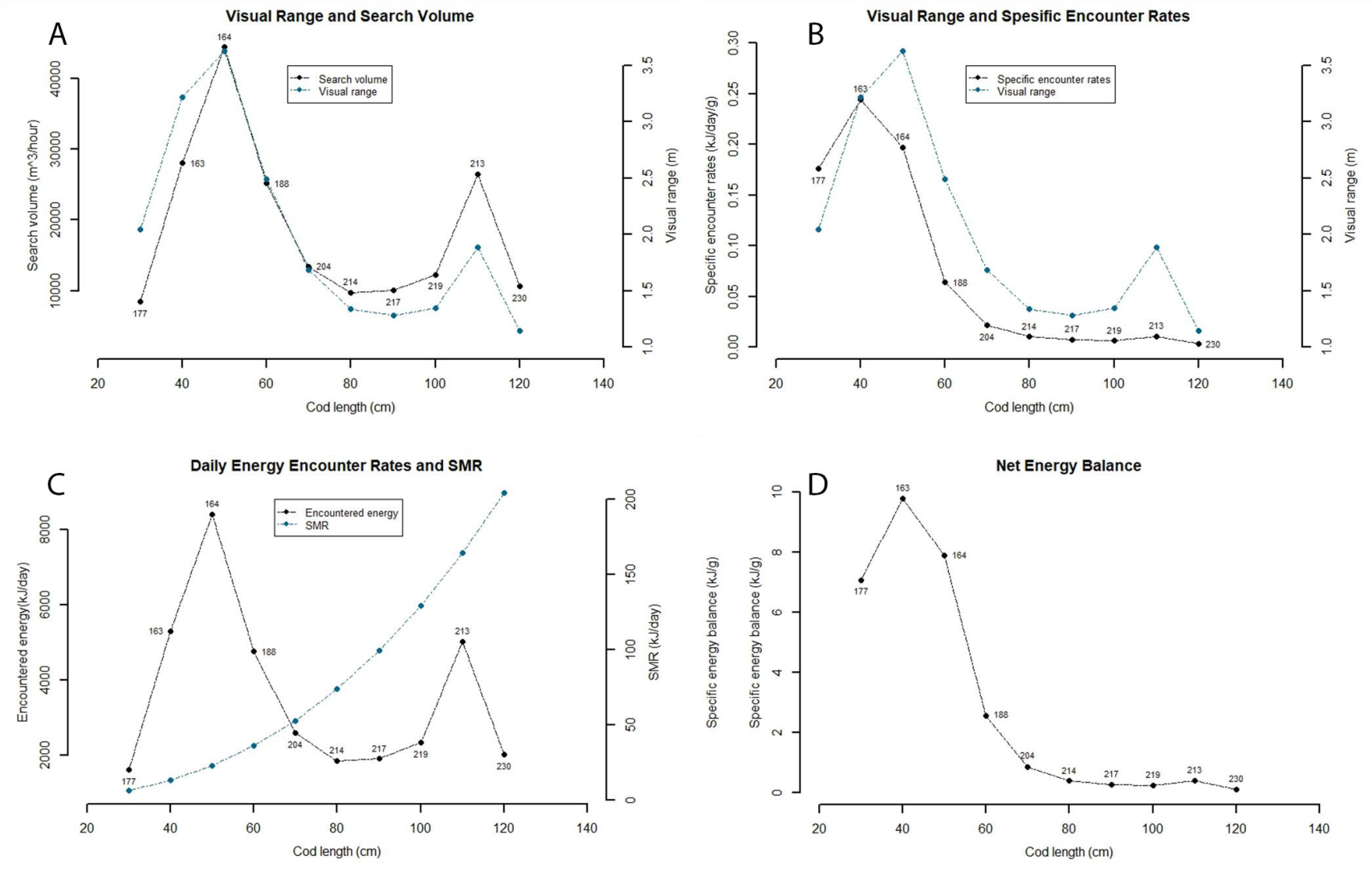
A
Visual Range and Search Volume
Search volume
Visual range
Search volume (m^3/hour)
Visual range (m)
Cod length (cm)
B
Visual Range and Spesific Encounter Rates
Specific encounter rates
Visual range
Specific encounter rates (kJ/day/g)
Visual range (m)
Cod length (cm)
C
Daily Energy Encounter Rates and SMR
Encountered energy
SMR
Encountered energy(kJ/day)
SMR (kJ/day)
Cod length (cm)
D
Net Energy Balance
Specific energy balance (kJ/g)
Specific energy balance (kJ/g)
Cod length (cm)

Figure 9. Visual range, encounter rates, search volume and SMR have been estimated for the average depths (numbers inserted close to the dots.) The median length group (30 cm for length group 25-34 cm, 40 cm for length group 35-44 cm etc.) has been used to predict values for each length Panel A) The visual range predicted by the model and hourly search volume based on that visual range. Panel B) The visual range from panel A compared to specific encounter rates (capelin day^{-1} g^{-1}.) Body weight was calculated using Eq. 10. Panel C) The daily energy encountered for each length group and their daily standard metabolic rates (SMR). SMR has been calculated from Eq. 12. Panel D) The net specific energy balance (kJ g^{-1}) for each length group.

The visual range at the average depth for each length group (Figure 7) is presented in Figure 9, along with the hourly search volume (panel A.) Visual range is estimated using Eq. 4, with irradiance at depth estimated using Eq. 7 with E_0=59 μmol m^{-2} s^{-1} and K=0.08 m^{-1}. Search volume is estimated using Eq. 2, but without the prey abundance parameter (N). The fact that the visual range plots lie higher than the search volume values for the two smallest length groups but lower for length groups >70 cm can be caused by the increase in swimming speed as cod grow larger.

The specific encounter rates (encounter rate per gram weight) predicted by my calculations decreases with size and depth (Figure 9, panel B.) Changes in depth influence specific encounter rates less as cod become larger, due to the weight parameter. This can be seen for the median for length group 105-114 cm (110 cm) where visual range increases a great deal while specific encounter rates remain more stable. This is not unexpected as relatively small increases in length causes progressively larger increases in weight as cod grow longer. The increase in visual range then becomes less significant compared to the weight for the larger cod than the smaller ones.

As cod grow larger and venture deeper, the model predicts that the absolute and relative amount of energy they encounter (in the form of prey encounter rates) decreases, even with the added benefit of larger eyes (Figure 9, panel C.) The energy encountered is calculated based on encounter rates and the energy density of the capelin. Encounter rates are estimated from Eq. 3 and SMR is estimated from Eq. 12. Energy per capelin is based on a 10 cm capelin weighing 5 g with an energy density of 8.05 kJ g^{-1}. Note that the scale on the y-axes are different (panel C) and that all cod are able to encounter more energy than their SMR at their average depth. The net energy balance (Figure 9, panel D) shows that, *ceteris paribus*, it is energetically better to stay shallower where the smaller length groups are, than at the depths where the larger length groups are, even with the benefits of larger eyes. It should be noted that energy requirements due to activity levels, growth and reproduction have not been included

4. Discussion

4.1 Heincke´s Law and The NEAC

The NEAC seem to obey Heincke´s law, showing an increase in depth as the size and age increases (Table 3 and Figure 6 and 7.) From Figure 6 and Table 3 it also becomes apparent that most cod prefer depths between ~100-300 m. The average depth range remains fairly constant for all length groups (Table 3.) This implies that the NEAC does not expand its depth range as it grows larger, but simply moves it deeper. The deepening between the smallest and largest length group was 53 m, while the maximum deepening (between length group 35-44 cm and 115-124 cm) was 67 m. . The NEAC show approximately the same deepening then as found for Atlantic cod in the Gulf of Maine (Methratta and Link, 2007, 50-100 m for 1->80 cm long cod) but less than found on the Scotian Shelf (Frank, *et al*., 2018, 80 m for age groups 4-12 (corresponds roughly to 50-110 cm) and in the Gulf of St. Lawrence (Swain, 1993, Tremblay and Sinclair, 1984, 160-260 m for age groups 3-8 years old (corresponds roughly to 40-90 cm.)) While it is impossible for me to do precise comparisons between my length groups and the age groups used in some of these articles, work done by Marteinsdottir and Begg (2002) suggests that 4-12 year old's corresponds roughly to 50-110 cm while 3-8 year old´s corresponds roughly to 40-90 cm. As the Gulf of Maine, Scotian Shelf and Gulf of St. Lawrence all show an average depth that is shallower than the Barents Sea (139 m, 90 m and 152 m respectively, versus 230 m) it is unlikely this is an artefact of available depths, but rather a response of the cod to some factor(s).

4.2 Lens Size-Body Length Relationship

My data suggest that there exists a positive, linear correlation between lens size and length (Figure 3.) This is congruent with other studies done on the eye and visual system in cod (Herbert, Steffensen and Jordan, 2004; Sadler, 1973) and is to be expected. A benefit of larger lenses is that they allow the cod to utilize more of the available light and therefore improve visual sensitivity and range, as have been shown in this thesis (Figure 8.) However, the benefits might go beyond this. Larger lenses have also been shown to improve resolution in the African cichlid fish (*Haplochromis burtoni*, Fernald and Wright, 1985) and sunfish (*Lepomis* spp.,

Walton *et al*., 1994) Enhanced acuity might help larger Atlantic cod hunt more efficiently, by improving prey recognition. This could in turn increasing encounter- and feeding rates. To confirm this for Altantic cod, laboratory experiments would have to be conducted to investigate, first, the effect increased lens size has on acuity and second, the effect improved acuity could have on prey recognition and feeding rates.

As even the smallest length groups of the NEAC are found at depths >200 m (Table 3), this indicates that they have exceedingly light sensitive eyes even at this size. Meager *et* al. (2010) showed that juvenile Atlantic cod (17-22 cm standard length) could see prey at light levels of 0.01 μmol m^{-2} s^{-1} (corresponding to 108 m depth with my irradiance (pE_0=59 μmol m^{-2} s^{-1}) and turbidity (K=0.08 m^{-1}) levels) and probably even lower than this. There is a possibility however, that this is an artefact of sampling (Johannesen, pers. com.) As the trawl is being brought to the surface, it can catch some individuals on the way, skewing the data.

4.3 Encounter Rates With Increased Lens Size and Depth

Given the parameters I have used for the visual range model and the average depth for each length group, the predicted encounter rates seem to decrease as cod grow larger. While increased lens size does increase visual range *ceteris paribus* (Figure 8), the visual range, search volume and encountered energy decrease with size when average depth is taken into (Figure 9.) Daily encounter rates between the smallest length group and the largest do actually increase (from about 10.2 to 12.7 capelin day^{-1}, Appendix, Figure A5) but this increase is insignificant. When lengths reach >80 cm, the negative effect of depth seems to become somewhat reduced with regards to visual range, search volume and encounter rates. This could indicate that for these sizes, the increase in lens size can compensate somewhat for the loss of light. The compensation is weak however and can only work as the average deepening between these length groups is notably smaller compared to length groups <80 cm. It seems then that light levels due to average depth has a much stronger influence on the visual range and encounter rates than does lens size due to increased body length. This is probably caused by the fact that light levels decrease exponentially with depth, while swimming velocity and visual range increases more or less linearly.

4.4 Limitations of The Data and The Model

While I have investigated the depth preferences for different length groups, no attempt has been made to establish the spatial distribution of length groups across the Barents Sea. As can be seen from Figure 1, the Barents Sea is shallower East and Northeast for Svalbard and West and Northwest of Novaya Semlya (≤200 m.) Comparing the depth profile of the Barents Sea to the abundance of NEAC in autumn 2013 (Ingvaldsen *et al*., 2015, Figure 1c) concentrations seem to be higher in these areas. The central part of the sea is for the most part deeper (≥400 m) and here abundances were several times lower compared to the shallower areas. Johannesen *et* al. (2012) also found a negative link between NEAC abundance and depth, at least for individuals >30 cm in length. The NEAC show both latitudinal and longitudinal spatial variation depending on age and season. 1-3 year old's are usually concentrated in the southeastern Barents Sea and along the polar front, while the mature specimens are found further south (Jakobsen and Ozhigin, 2011, p. 230.) As there almost certainly exists a relationship between spatial and bathymetric distribution, combining longitudinal and latitudinal location with average depth could possible elucidate novel patterns.

It should be noted that my sample size on length vs lens size was rather small (21 individuals) so the linearity of the lens size-to-length relationship might be misleading. My length data is also calculated from the head sizes I had, meaning that there is uncertainties connected with the length estimates as well. Sampling more cod over a larger length range than I have and correlating lens size to *actual* body lengths would give a more robust and accurate representation of the relationship between eye size and size for this species.

A fair amount of assumptions have been made when calculating the visual range and encounter rates. Especially the ΔS_e (irradiance sensitivity measured at the cornea) and ΔS_r (irradiance sensitivity measured at the retina) parameters have a large amount of uncertainty associated with them. I have calculated ΔS_r based on an *f* value (focal length) that corresponds to the smallest eye size calculated in my thesis (lens radius=2.49 mm) and I have kept it constant for all calculations. This assumption might be flawed, as it is possible for ΔS_r to change as the cod grows larger. There has been some indication that contrast threshold (which corresponds to the ΔS_r parameter) decreases as Atlantic cod grow larger (Anthony, 1981) but too little data was available to test for statistical significance. Research done on other species indicate the same, including goldfish (*Carrasius auratus*, Hester, 1968) and saithe (*Pollachius virens*, Protasov, 1970) and it is believed that visual acuity and sensitivity increases for

several species of fish as the size of the eye increases (Lyall, 1957; O´Connell, 1963; Tamura, 1957.) It is therefore quite possible that the retinal sensitivity of the Atlantic cod increases as the fish grows larger. If this is the case, this causes a further decrease in the irradiance sensitivity at the cornea (ΔS_e) with increased lens size, which would entail longer visual range and higher encounter rates as the fish grows. This added visual range could perhaps be sufficient to compensate for the decrease in light with depth.

The change in diet with age has not been taken into account either. Atlantic cod <2 years eat mostly krill and amphipods while older individuals forage mostly for fish (Dalpadado and Bogstad, 2004.) This could lead to a change in both prey size (A_p) and contrast (C_0) as the main prey changes (the effect of prey size on visual range can be found in Appendix, Figure A2.) Scharf, Juanes and Rountree (2000) showed that maximum prey size increased as the Atlantic cod grew larger, but the minimum size remained fairly constant. Larger cod could therefore have a broader range of prey sizes to choose from, compared to smaller conspecifics. This improves chances of satisfying their energy needs in three ways: 1) as there is more available prey, the effective prey density increases. 2) the increase in prey size effectively increases visual range and encounter rates. 3) Due to the square-cube law, the mass (volume) of the prey would increase exponentially as the size (area) increased. This can lead to higher energy content per encounter for larger cod. The density of larger prey is however probably lower than for smaller prey, which may offset this potential benefit, but it is likely that factors such as this influences foraging success for the NEAC at different depths.

Also, location (along with season) affects prey choice. During autumn, cod feed on polar cod in the Eastern part of the Barents Sea, while they feed primarily on capelin in the Northwestern part (Jakobsen and Ozhigin, 2011, p. 238.) This thesis has also assumed that vision is the primary sense used for foraging. Atlantic cod have a large eyes and well developed optic lobes (Kotrschal, Van Staaden and Huber, 1998) but they also have other sensory organs that have are linked to foraging. Atlantic cod exhibit highly sensitive olfactory organs (Johnstone, 1980), cutaneous taste buds on the head and fins (Harvey and Batty, 2002) and laboratory experiments have shown that they use both olfaction and taste buds on the barbel and pelvic fins to detect food (Brawn, 1969.) Hence, it is possible that Atlantic cod use these senses to detect prey at greater distances and that the visual sense only becomes important when the prey is within striking distance. Very little work is done on the hunting tactics of large cod (>50 cm) however, so this would only be speculative at this point.

4.5 Alternative Explanations for Heincke´s Law

Another physiological structure, other than the eye, that might affect depth distribution is the swim bladder. Cod are physoclists, which means that they cannot ascend or descend to rapidly without gaining or losing buoyancy (Stensholt *et al.*, 2002). As the cod grows, so does the swim bladder, which could mean that it would take longer for a large cod to reach neutral buoyancy at a new depth than a smaller one. Stenholt *et al.* showed that physoclists have a free vertical range (FVR) which is a vertical zone that they can ascend and descend within without becoming over- or under-buoyant. As pressure increases at a constant rate with depth, the relative increase in pressure from one depth to another decreases. It is therefore possible that the increase in average depth is caused by the need to have lower relative increases and decreases in pressure as they move up and down in the water column. This hypothesis would need to be tested, as no one has yet linked the expansion and compression of the swim bladder to ontogenetic deepening.

A lot of the hypotheses proposed for ontogenetic deepening in Atlantic cod and other fish species are based on sound ecological and/or physiological responses to different factors such as predation, competition or temperature. Lower predation levels have been linked to shallower areas, especially for juvenile Atlantic cod (Linehan, Gregory and Schneider, 2001; Gorman, Gregory and Schneider, 2009) and Ryer, Laurel and Stoner (2010) also used predation as an explanation for why juvenile flatfish prefer shallower waters. The problem with these hypotheses with regards to the NEAC is that 1) they have been looking at 0-group, year-1, year-2 and year-3 groups. Anything smaller than year-2 groups have been excluded from my thesis due to their poor catchability, which makes comparisons weak. 2) the depths they have sampled are much shallower than mine (1-20 m.) Topographical complexity and/or macroalgea densities are factors used to explain why smaller individuals prefer shallower waters and I have no reason to expect large changes in these factors across the average depths I found for the NEAC. Macroalgea growth is also just found in the shallowest parts of the Barents Sea.

Different sensitivities to competition with age and size could perhaps account for the ontogenetic deepening pattern for the NEAC. When abundance was high, the density of older (and larger) cod was found to be higher in deeper waters in the Gulf of St. Lawrence (Swain, 1993.) As the spawning stock biomass of cod in the Barents Sea is at or close to an all time high (Kjesbu *et al.*, 2014) this could lead to relative high density levels and perhaps influence

depth preference. Why this density dependent ontogenetic deepening only should affect the larger individuals is however unclear. Perhaps different length groups have different density tolerance levels. Off the South West coast of Ireland, scientists found a significant increase in size for scavenging fish with depth (Collins *et al.*, 2005). The pattern was also evident in some of the non-scavenging species, but it was less predominant. The argument for increased size with depth for scavenging species was that larger individual can collect and store more energy from a meal than a smaller conspecific, along with having a lower specific metabolic rate and swimming costs. This reduces the risk of starving while swimming between food sources means the larger individuals can exploit a niche that is out of reach for smaller individuals as the meals are too widely spaced. Since I have not investigated the capelin density with depth in this thesis, I cannot conclude nor deny that this affects depth preference in cod. I will however state that as the NEAC is primarily a predator, the distribution of prey might not be as influenced by depth as with scavengers, although it is very resonable to assume that prey densities do decrease with depth for cod as well.

As most teleosts are ecthotermic, temperature has a significant influence on their distribution and metabolic rate (Clarke and Johnston, 1999.) One study done on ontogenetic deepening concluded that ontogenetic deepening was likely caused by the larger fish benefiting from longer lives and reduced metabolism at the lower temperatures experienced in deeper waters (MacPherson and Duarte, 1991.) The smaller individuals would gain accelerated growth rates at shallower depths which would decrease time spent in size groups that experience high predation rates. A difference in temperature preferences with age (and size) has been demonstrated for several species of fish in several geographic locations (Gibson *et al.*, 2002; Kwain and McCauley, 2011; McCauley and Read, 2011) and provides creedence to this hypothesis. A thermal preferendum experiment conducted in 2005 showed that Atlantic cod prefer cooler temperatures as they grow larger (Lafrance *et al.*, 2005) and that the smallest individuals (fork length ~10 cm) occupied a portion of the tank that was more than twice as warm as the largest individuals (fork length >60 cm.) Another experiment looked at growth rates for different sized cod depending on temperature (Árnason, Björnsson and Steinarsson, 2009). Smaller cod seemed to thrive in warmer waters, gaining more weight here than in colder conditions. Larger cod prefered intermediate or cold temperatures. I did also find a similar pattern, indicating that larger individuals prefered colder waters (Appendix, Figure A4.) However, I also found that temperature varied noticeably across depth ranges (Appendix, Figure A1.) The difference in temperature between maximum and minumum temperature is

less then 1º C for the entire depth range relevant to this thesis (150-250 m.) By contrast, change in temperature is much larger depending on where in the Barents Sea the cod is located. In September, bottom temperatures drop progressively further North and Northeast from the Norwegian coast, from around 6-4ºC down to -2ºC in some areas (Jakobsen and Ozhigin, 2011, p. 53.) But as both temperature and geographical location are confounding factors influencing depth preference, more thorough statistical analyses are needed.

Last year an article was published indicating that ontogentic deepening could be an artifact of fishing (Frank *et al.*, 2018). Virtually all species that fit the pattern are commercially harvested. However, few or none have looked at the effects fishing could have on depth distribution. This implies that we may have been looking for ecological and physiological explanations to a pattern that is mostly driven by human exploitation. Although I have not tested this hypothesis for the NEAC, it is much less stationary than the stock used in Frank *et al.´*s article (the eastern Scotian Shelf cod.) Seasonal migrations would likely therefore "repopulate" areas of low densities due to fishing. The fishing in the Barents Sea is also seasonal and much of it is located along the coasts (Jakobsen and Ozhigin, 2011, p. 617.) This then, means that fishing induced ontogenetic deepening is less probable for the NEAC, although it cannot be ruled out.

In a reply to Frank *et al.´*s article, Audzijonyte and Pecl (2018) suggested how different drivers could produce depth distributions that would lead to real or apparent ontogenetic deepening. Depending on the factor behind the pattern, the distribution of the different length groups in the water column should change. If predation is the principle driver, then the expected pattern would be that the abundance of smaller individuals is greatest in shallower waters, becoming reduced with depth. This could be caused either by smaller individuals moving to shallower areas to avoid predators or simply being eaten at greater depths. If competition in shallower areas has a disproportionate effect on larger individuals compared to smaller ones, a pattern where densities of larger individuals increases with depth is expected. Should temperature be influencing depth preference, either of the two patterns, or a combination, could be present. Finally, if fishing is the major driver for ontogenetic deepening in the NEAC then a pattern of low abundance of large individuals in shallower waters, accompanied with an increase in abundance with increasing depth, should be present. From my data, there is no sudden reduction of smaller individuals with increasing depth, nor is there a sudden increase in larger individuals. This makes it hard to argue for any of the proposed explanations presented here.

5. Conclusion

The ontogenetic deepening observed for Atlantic cod elsewhere is present in the Barents Sea, but what factors drive this pattern for the NEAC is still unclear. The depth preferences found in this thesis also only tell a part of the story. Linking it with latitudinal and longitudinal data could give a more complete image of spatial distribution and provided a three dimensional picture of where the different length groups of the NEAC are found. Adding data on temperature and geographic distribution of prey could further elevate the usefulness of such studies. Such a combination of data could help management as it would give a more precise picture of how the NEAC is distributed and perhaps why. This might help improve management by more accurately pinpointing areas of high densities for different sizes (and ages) of this stock. It could also help fisheries more accurately target areas with strong year classes, which can lead to more predictable yearly landings while maintaining a sustainable fishery.

While increased eye size is bound to have a positive kurlansk balance, Figure 9, panel D) is drastically reduced as cod grow larger and venture deeper, implying an evolutionary cost of occupying deeper waters. I would assume that there exists some other benefit for larger cod at greater depths, but is has not been discovered by this thesis. There are perhaps other variables that change as cod venture deeper, like hunting tactics or prey choice that have not been addressed here.

This thesis´ inability to explain what drives ontogenetic deepening in the NEAC could be caused by investigating the wrong factor(s). Or it could be related to not accounting for confounding variables such as temperature, geographic location, diet or other, unknown factors. It goes to show the importance of understanding the intricate relationships between physical and biological factors and how they together can shape distributions.

.

6. References

Aksnes, D. L. and Giske, J. (1993) 'A theoretical model of aquatic visual feeding', *Ecological Modelling*, 67(2-4), pp. 233-250. doi: 10.1016/0304-3800(93)90007-F.

Aksnes, D. L. and Utne, A. C. W. (1997) 'A revised model of visual range in fish', *Sarsia*, 82(2), pp. 137–147. doi: 10.1080/00364827.1997.10413647.

Anthony, P. D. (1981) 'Visual contrast thresholds in the cod Gadus morhua L.', *Journal of Fish Biology*, 19(1), pp. 87–103. doi: 10.1111/j.1095-8649.1981.tb05814.x.

Árnason, T., Björnsson, B. and Steinarsson, A. (2009) 'Allometric growth and condition factor of Atlantic cod (Gadus morhua) fed to satiation: Effects of temperature and body weight', *Journal of Applied Ichthyology*. doi: 10.1111/j.1439-0426.2009.01259.x.

Audzjionyte, A. and Pecl, G. T. (2018) 'Deep impact of fisheries', *Nature Ecology and Evolution*, 2, pp. 1348-1349. doi: 10.1038/s41559-018-0653-9.

Bakketeig I.E., Hauge M. og Kvamme C. (red). 2017 Havforskningsrapporten 2017. Fisken og havet, særnr. 1–2017.

Barten, P. G. J. (1992) 'Physical model for the contrast sensitivity of the human eye', *Human Vision, Visual processing and Digita Display III*, 1666, pp. 57-72. doi: 10.1117/12.135956.

Beer, A. (1852) 'Bestimmung der Absorption des rothen Lichts in farbigen Flussigkeiten', *Ann. Physik*, 162(), pp. 78-88.

Björnsson, B. (1993) 'Swimming speed and swimming metabolism of Atlantic cod (Gadus morhua) in relatio to available food: A laboratory study', *Canadian Journal of Fisheries and Aquatic Sciences*. doi: 10.1139/f93-277.

Bowmaker, J. K. (1995) 'The Visual Pigments in Fish', *Progress in Retinal and Eye Research*, 15(1), pp. 1-31. doi: 10.1016/1350-9462(95)00001-1.

Bowmaker, J. K. (2008) 'Evolution of vertebrate visual pigments', *Vision Research*, 48(20), pp. 2022–2041. doi: 10.1016/j.visres.2008.03.025.

Brawn, V. M. (1969) 'Feeding behaviour of cod (Gadus morhua)', *Journal of the Fisheries Reasearch Board of Canda*, 26(3), pp. 583-596. doi: 10.1139/f69-05.

Clarke, A. and Johnston, N. M. (1999) 'Scaling of metabolic rate with body mass and temperature in teleost fish', *Journal of Animal Ecology*. doi: 10.1046/j.1365-2656.1999.00337.x.

Collin, S. P. and Marshall, N. J. (2003) 'Retinal Sampling and the Visual Field in Fishes', in *Sensory Processing in Aquatic Environments*, p. 446. doi: 10.1007/b97656.

Collins, M. A. *et al.* (2005) 'Trends in body size across an environmental gradient: A differential response in scavenging and non-scavenging demersal deep-sea fish', *Proceedings of the Royal Society B: Biological Sciences*. doi: 10.1098/rspb.2005.3189.

Dalpadado, P. and Bogstad, B. (2004) 'Diet of juvenile cod (age 0-2) in the Barents Sea in relation to food availability and cod growth', *Polar Biology*, 27(3), pp. 140–154. doi: 10.1007/s00300-003-0561-5.

Dolgov, A. V. (2002) 'The role of capelin (Mallotus villosus) in the foodweb of the Barents Sea', in *ICES Journal of Marine Science*. doi: 10.1006/jmsc.2002.1237.

Dunbrack, R. L. and Dill, L. M. (1984) 'Three-Dimensional Prey Reaction Field of the Juvenile Coho Salmon (Oncorhynchus kisutch)', *Canadian Journal of Fisheries and Aquatic Sciences*, 41(8), pp. 1176-1182. doi: 10.1139/f84-139.

FAO (2018) *The State of World Fisheries and Aquaculture 2018 - Meeting the sustainable development goals*. Rome: UN.

Fernald, R. D. and Wright, S. E. (1985) ' Vision and behavior in an African cichlid fish (*Haplochromis burtoni*): Optics', *Vision Research*, 25(2), pp. 155-161. doi: 10.1016/0042-6989(85)90108-7.

Luna, S. M. and Valdestamon, R. R. (2018) *Mallotus villosus* (Müller, 1777) [Internett]. Available from https://www.fishbase.se/summary/Mallotus-villosus# [Read 13th of October, 2018]

Frank, K. T. *et al.* (2018) 'Exploitation drives an ontogenetic-like deepening in marine fish', *Proceedings of the National Academy of Sciences*, 115(25), pp. 6422–6427. doi: 10.1073/pnas.1802096115.

Gagnon, Y. L., Sutton, T. T. and Johnsen, S. (2015) 'Visual acuity in pelagic fishes and mollusks', *Vision Research*, 92, pp. 1–9. doi: 10.1016/j.visres.2013.08.007.

Galloway, T. F., Kjørsvik, E. and Kryvi, H. (1998) ‘Effect of temperature on viability and axial muscle development in embryos and yolk sac larvae of the Northeast Arctic cod (Gadus morhua)’, *Marine* Biology, 132(4). pp. 559-567. doi: 10.1007/s002270050421.

Gibson, R. N. *et al.* (2002) ‘Ontogenetic changes in depth distribution of juvenile flatfishes in relation to predation risk and temperature on a shallow-water nursery ground’, *Marine Ecology Progress Series*. doi: 10.3354/meps229233.

Gjertsen, K. E., and Ingvaldsen, R. 2018. Map of currents in the Barents Sea. Institute of Marine Research.

Gjøsæter, H. (1998) ‘The population biology and exploitation of capelin (Mallotus villosus) in the barents sea’, *Sarsia*, 83(6), pp. 453-496. doi: 10.1080/00364827.1998.10420445.

Gorman, AM., Gregory, R. S. and Schneider, D. C. (2009) ‘Eelgrass patch size and proximity to the patch edge affect predation risk of recently settled age 0 cod (Gadus)’, 371(1), pp. 1-9. doi: 10.1016/j.jembe.2008.12.008.

Gorman, O. T. (1987) ‘Habitat segregation in an assemblage of minnows in an Ozark stream’, in *Community and Evolutionary Ecology of North American Stream Fishes*.

Gregg, W. W. and Carder, K. L. (1990) ‘A simple spectral solar irradiance model for cloudless maritime atmospheres’, *Limnology and Oceanography*, 35(8), pp. 1657–1675. doi: 10.4319/lo.1990.35.8.1657.

Greivenkamp, J. E., Schwiegerling, J., Miller, J. M. and Mellinger, M. D. (1995) ‘Visual acuity modeling using optical raytracing of schematic eyes’, *American Jurnal of Opthalmology*, 120(2), pp. 227-240. doi: 10.1016/S0002-9394(14)72611-X.

Hamre, J. (1994) ‘Biodiversity and exploitation of the main fish stocks in the Norwegian - Barents Sea ecosystem’, *Biodiversity and Conservation*, 3(6), pp. 473-492. doi: 10.1007/BF00115154.

Hamre, J. (2003) ‘Capelin and herring as key species for the yield of north-east Arctic cod. Results from multispecies model runs’, *Scientia Marina*, 67(S1), pp. 315-323. doi: 10.3989/scimar.2003.67s1315.

Harvey, B. C. and Stewart, A. J. (1991) ‘Fish size and habitat depth relationships in

headwater streams', *Oecologia*. doi: 10.1007/BF00634588.

Harvey, R. and Batty, R. S. (2002) 'Cutaneous taste buds in gadoid fishes', *Journal of Fish Biology*, 60(3), pp. 583–592. doi: 10.1006/jfbi.2002.1875.

Heincke, F. (1913) 'Investigations on the plaice', *General report 1. Rapports et Procès- Verbaux des Réunions (International Council for the Exploration of the Sea, Copenhagen).*

Herbert, N. A., Steffensen, J. F. and Jordan, A. D. (2004) 'The interrelated effects of body size and choroid rete development on the ocular O2 partial pressure of Atlantic (Gadus morhua) and Greenland cod (Gadus ogac)', *Polar Biology*, 27, pp. 748-752. doi: 10.1007/s00300-004-0657-6.

Hester, F. (1968) 'Visual contrast thresholds of the goldfish (Carassius auratus)', *Vision Research*, 8(10), pp. 1315-1336. doi: 10.1016/0042-6989(68)90053-9.

Ingvaldsen, R. B. *et al*. (2015 'Modelled and observed cod distributions', *Nature Climate Change*, 5, pp. 1-4. doi:

Jagger, W. S. (1992) 'The optics of the spherical fish lens', *Vision Research*, 32(7), pp. 1271–1284. doi: 10.1016/0042-6989(92)90222-5.

Jakobsen, T and Ozhigin, V. K. (2011) 'The Barents Sea; Ecosystem, Resources, Management; Half a century of Norwegian-Russian cooperation', Trondheim: Tapir Academic Press.

Johannesen, E., Johansen, G. O., and Kursbrekke, K. (2015) 'Seasonal variation in cod feeding and growth in a changing sea', *Canadian Journal of Fisheries and Aquatic Sciences*, 73(2), pp. 235-245. doi: 10.1139/cjfas-2015-0052.

Johannesen, E., Lindstrøm, U., Michaelsen, K., Skern-Mauritzen, M., Fauchald, P., Bogstad, B. and Dolgov, A. (2012) 'Feeding in a heterogeneous environment: Spatial dynamics in summer foraging Barents Sea cod', *Marine Ecology Progress Series*, 458, pp. 181-197. doi: 10.3354/meps09818.

Johnstone, A. D. F. (1980) 'The detection of dissolved amino acids by the Atlantic cod, Gadus morhua L.', *Journal of Fish Biology*, 17, pp. 219-230. doi: 10.1111/j.1095-8649.1980.tb02755.x.

Jørgensen, C. and Fiksen, Ø. (2006) ‘State-dependent energy allocation in cod (*Gadus morhua*)’, *Canadian Journal of Fisheries and Aquatic Sciences*, 63(1), pp. 186-199. doi: 10.1139/f05-209.

Karamushko, L. I. (2001) ‘Metabolic Adaptation of Fish at High Latitudes’, *Doklady Biological Science*, 379, pp. 359-361.

Kjesbu,O. S., Bogstad, B., Devine, J. A., Gjøsæter, H., Howell, D., Ingvaldsen, R. B.,Nash, R. D. M. and Skjæraasen, J. E. (2014) ‘Synergies between climate and management for Atlantic cod fisheries at high latitudes’, *Proceedings of the National Academy of Sciences*, 111(9), pp. 3478-3483. doi: 10.1073/pnas.1316342111.

Kotrschal, K., Van Staaden, M. J. and Huber, R. (1998) ‘Fish brains: Evolution and environmental relationships’, *Reviews in Fish Biology and Fisheries*, 8(4), pp. 373–408. doi: 10.1023/A:1008839605380.

Kurlansky, M. (1999) ‘Cod: a biography of the fish that changed the world’, New York: Vintage Publishing.

Kwain, W.-H. and McCauley, R. W. (2011) ‘ Effects of Age and Overhead Illumination on Temperatures Preferred by Underyearling Rainbow Trout, Salmo gairdneri , in a Vertical Temperature Gradient ’, *Journal of the Fisheries Research Board of Canada*. doi: 10.1139/f78-225.

Lafrance, P. *et al.* (2005) ‘Ontogenetic changes in temperature preference of Atlantic cod’, *Journal of Fish Biology*. doi: 10.1111/j.0022-1112.2005.00623.x.

Laurel, B. J., Gregory, R. S. and Brown, J. A. (2003) ‘Predator distribution and habitat patch area determine predation rates on Age-0 juvenile cod Gadus spp.’, *Marine Ecology Progress Series*, 251, pp. 245-254. doi: 10.3354/meps251245.

Linehan, J. E., Gregory, R. S. and Schneider, D. C. (2001) ‘Predation risk of age-0 cod (Gadus) relative to depth and substrate in coastal waters’, *Journal of Experimental Marine Biology and Ecology*. doi: 10.1016/S0022-0981(01)00287-8.

Loeng, H. (1991) ‘Features of the physical oceanographic conditions of the Barents Sea’, *Polar Research*, 10(1), pp. 5-18. doi: 10.3402/polar.v10i.6723.

Lueck, C. and O´Brien, W. J. (1981) ‘Prey Location Volume of a Planktivorous Fish:

A New Measure of Prey Vulnerability', *Canadian Journal of Fisheries and Aquatic* Sciences, 38(10), pp. 1264-1270. doi: 10.1139/f81-168.

Lyall, A. H. (1957) 'The Growth of the Trout Retina', *Journal of Cell Science*, 3(98), pp. 101-110.

Lythgoe, J. N. (1988) 'Light and Vision in the Aquatic Environment', *Sensory Biology of Aquatic Animals*, New York; Springer.

Macpherson, E. and Duarte, C. M. (1991) 'Bathymetric trends in demersal fish size: is there a general relationship?', *Marine Ecology Progress Series*, pp. 103–112. doi: 10.3354/meps071103.

Marteinsdottir, G. and Begg, G. A. (2002) 'Essential relationships incorporating the influence of age, size and condition on variables required for estimation of reproductive potential in Atlantic cod Gadus morhua', *Marine Ecology Progress* Series, 235, pp. 235-256. doi: 10.3354/meps235235.

Matthiessen, L. (1882) 'Ueber die Beziehungen, welche zwischen dem Brechungsindex des Kerncentrums der Krystalllinse und den Dimensionen des Auges bestehen', *Pfl??ger, Archiv f??r die Gesammte Physiologie des Menschen und der Thiere*. doi: 10.1007/BF01802978.

McCauley, R. W. and Read, L. A. A. (2011) ' Temperature Selection by Juvenile and Adult Yellow Perch (Perca flavescens) Acclimated to 24 C ', *Journal of the Fisheries Research Board of Canada*. doi: 10.1139/f73-202.

Meager, J. J. *et al.* (2010) 'Effects of light intensity on visual prey detection by juvenile atlantic cod (Gadus morhua L.)', *Marine and Freshwater Behaviour and Physiology*, 43(2), pp. 99–108. doi: 10.1080/10236241003798910.

Methratta, E. T. and Link, J. S. (2007) 'Ontogentic variation in habitat association for four groundfish species in the Golf of Maine-Goerges Bank region', *Marine Ecology Progress Series*, 338, pp. 169-181. doi: 10.3354/meps338169.

Moranta, J. *et al.* (1998) 'Fish community structure and depth-related trends on the continental slope of the Balearic Islands (Algerian basin, western Mediterranean)', *Marine Ecology Progress Series*. doi: 10.3354/meps171247.

Munz F. W. and McFarland W. N. (1977) ‘Evolutionary Adaptations of Fishes to the Photic Environment’, *The Visual System in Vertebrates. Handbook of Sensory Physiology*, vol. 7 Berlin: Springer.

O´Connell, C. P. (1963) ‘The structure of the eye of *Sardinops caerulea, Engraulis mordax,* and four other pelagic marine teleosts’, *Journal of Morphology,* 113(2), pp. 287-329. doi: https://doi.org/10.1002/jmor.1051130214.

Olsen, E., Aanes, S., Mehl, S., Holst, J. C., Aglen, A. and Gjøsæter, H. (2009) ‘Cod, haddock, saithe, herring, and capelin in the Barents Sea and adjacent waters: A review of the biological value of the area’, *ICES Journal of Marine Science,* 78, pp. 87-101. doi: 10.1093/icesjms/fsp229

Ottersen, G. *et al.* (2014) ‘A review of early life history dynamics of Barents Sea cod (Gadus morhua)’, *ICES Journal of Marine Science*. doi: 10.1093/icesjms/fsu037.

Ottersen, G., Michalsen, K. and Nakken, O. (1998) ‘Ambient temperature and distribution of north-east Arctic cod’, *Ices Journal of Marine Science*, 55(1), pp. 67–85. doi: 10.1006/jmsc.1997.0232.

Phillips, D. and Kirk, J. (1984) ‘Study of the spectral variation of absorption and scattering in some australian coastal waters’, *Marine and Freshwater Research*, 35(6) pp. 635-644. doi: 10.1071/MF9840635.

Polloni, P. *et al.* (1979) ‘The Size-Depth Relationship in Deep Ocean Animals’, *Internationale Revue der gesamten Hydrobiologie und Hydrographie*, 64(1), pp. 39–46. doi: 10.1002/iroh.19790640103.

Power, M. E. (1984) ‘Depth distributions of armored catfish: predator-induced resource avoidance?’, *Ecology*. doi: 10.2307/1941414.

Protasov, V. R. (1970) ‘Vision and Near Orientation of Fish’, *Academy of Sciences of the USSR*, pp. 175.

Ryer, C. H., Laurel, B. J. and Stoner, A. W. (2010) ‘Testing the shallow water refuge hypothesis in flatfish nurseries’, *Marine Ecology Progress Series*. doi: 10.3354/meps08732.

Scharf, F., Juanes, F. and Rountree, R. (2000) ‘Predator size - Prey size relationships of marine fish predators: Interspecific variation and effects of ontogeny and body size on

trophic-niche breadth', *Marine Ecology Progress Series*, 208, pp. 229-248. doi: 10.3354/meps208229.

Sadler, J. D. (1973) 'The focal length of the fish eye lens and visual acuity', *Vision Research*, 13(2), pp. 417–423. doi: 10.1016/0042-6989(73)90118-1.

Sakshaug, E. and Slagstad, D. (1991) 'Light and productivity of phytoplankton in polar marine ecosystems: a physiological view', *Polar Research*. doi: 10.1111/j.1751-8369.1991.tb00636.x.

Schultz, L. P. (1937) 'Rediscription of the capelin *Mallotus catervarius* (pennant) of the North Pacific' *Proceedings of the United States National Museum*, 85, pp. 13-20.

Schwassmann, H. O. (1975) 'Vision in Fishes', vol 1. Boston, MA: Springer.

Skaret, G. Johannesen, E. Fall, J. and Fiksen, Ø. (2016) 'Survey report from the CODFUN 2016114 Barents Sea survey 5.-11. oktober 2016'. 41. Available from: https://brage.bibsys.no/xmlui/bitstream/handle/11250/2477070/Cruise%2breport%2bCODFUN_final%2beh%2b31.01..pdf?sequence=2&isAllowed=y [Read; 3rd of Febuary, 2019].

Smedsrud, L. H., *et al.* (2013) 'The role of the Barents Sea in the Arctic climate system', *Reviews of Geophysics*, 15, pp. 415-499. doi: 10.1002/rog.20017.

Snelgrove, P. and Haedrich, R. (1985) 'Structure of the deep demersal fish fauna off Newfoundland', *Marine Ecology Progress Series*, 27(June), pp. 99–107. doi: 10.3354/meps027099.

Sogard, S. M. (1997) 'Size-selective mortality in the juvenile stage of teleost fishes: A review', *Bulletin of Marine Science*.

Stensholt, B. K. *et al.* (2002) 'Vertical density distributions of fish: A balance between environmental and physiological limitation', *ICES Journal of Marine Science*. doi: 10.1006/jmsc.2002.1249.

Sternheim, M. M. S. and Kane, J. W. (1986) 'General physics' New York: John Wiley & Sons.

Swain, D. P. (1993) 'Age- and density-dependent bathymetric pattern of Atlantic cod (Gadus morhua) in the southern Gulf of St. Lawrence', *Canadian Journal for Fisheries and*

Aquatic Science, 50, pp. 1255-1264. doi: 10.1139/f93-142.

Tamura, T. (1957) ‘A study of visual perception in fish, especially on resolving power and accommodation’, *Nippon Suisan Gakkaishi*, 22, pp. 536-557. doi:

Thetmeyer, H. and Kils, U. (1995) ‘To see and not be seen: the visibility of predator and prey with respect to feeding behaviour’, *Marine Ecology Progress Series*. doi: 10.3354/meps126001.

Tremblay, M. J. and Sinclair, M. (1984) ‘Gulf of St, Lawrence cod: age-specific geographic distributions and environmental occurrences from 1971 to 1981’

Canadian Technicall Report of Fisheries and Aquatic Science, 1387, pp.

Walton, W. E. *et al*., (1994) ‘Size-related Change in the Visual Resolution of Sunfish (Lepomis spp.)‘, *Canadian Journal of Fisheries and Aquatic Sciences*, 51(9), pp. 2017-2026. doi: 10.1139/f94-204.

Yaragina, N. A., Aglen, A., and Sokolov, K. M. (2011). “Cod,” in *The Barents Sea, Ecosystem, Resources, Management. Half a Century of Russian–Norwegian cooperation*, eds. T. Jakobsen and V. K. Ozhigin (Trondheim: Tapir academic press).

Yaragina, ., Bogstad, . and Kovalev, . (2009) ‘Variability in cannibalism in Northeast Arctic cod (Gadus morhua) during the period 1947-2006’, *Marine Biology Research*, 5(1), pp. 75-85. doi: 10.1080/17451000802512739.

7. Appendix 1 – Additional Analyses and Graphs

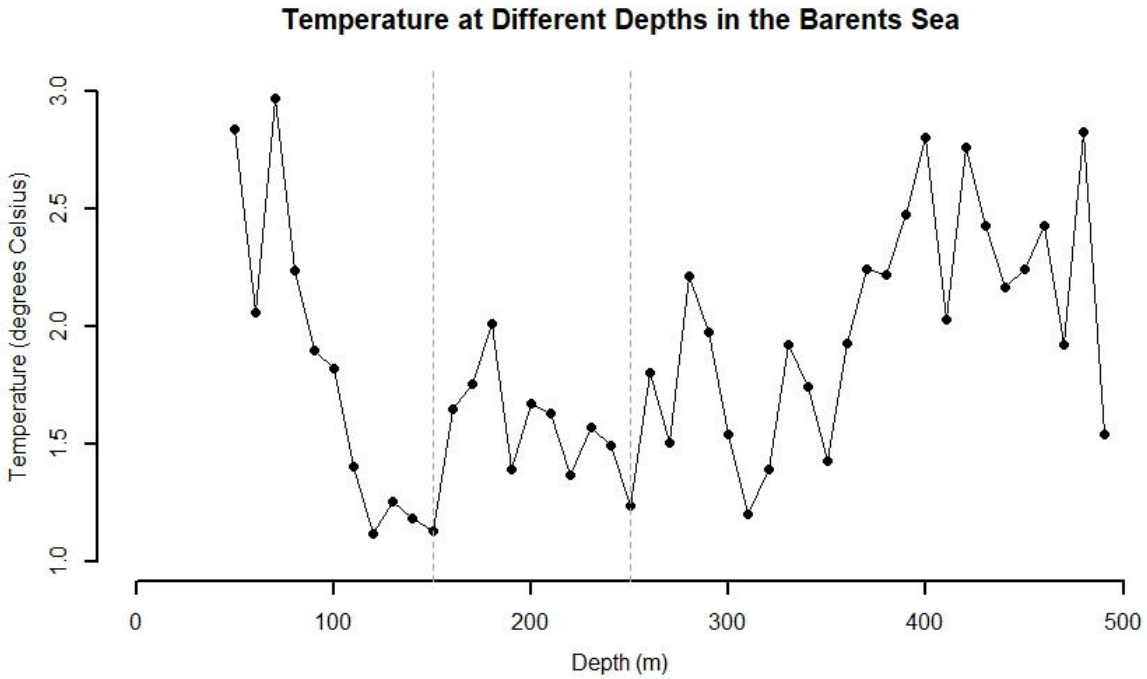

Figure A1. The average temperature over 10 m intervals through the water column in the Barents Sea, measured during the BESS. The dotted, grey lines represent the depth interval where the NEAC length groups where found in this thesis, ~150-250 m. The linear regression analysis showed a weak, near-significant correlation between depth and temperature (R^2=0.064, p=0.052.)

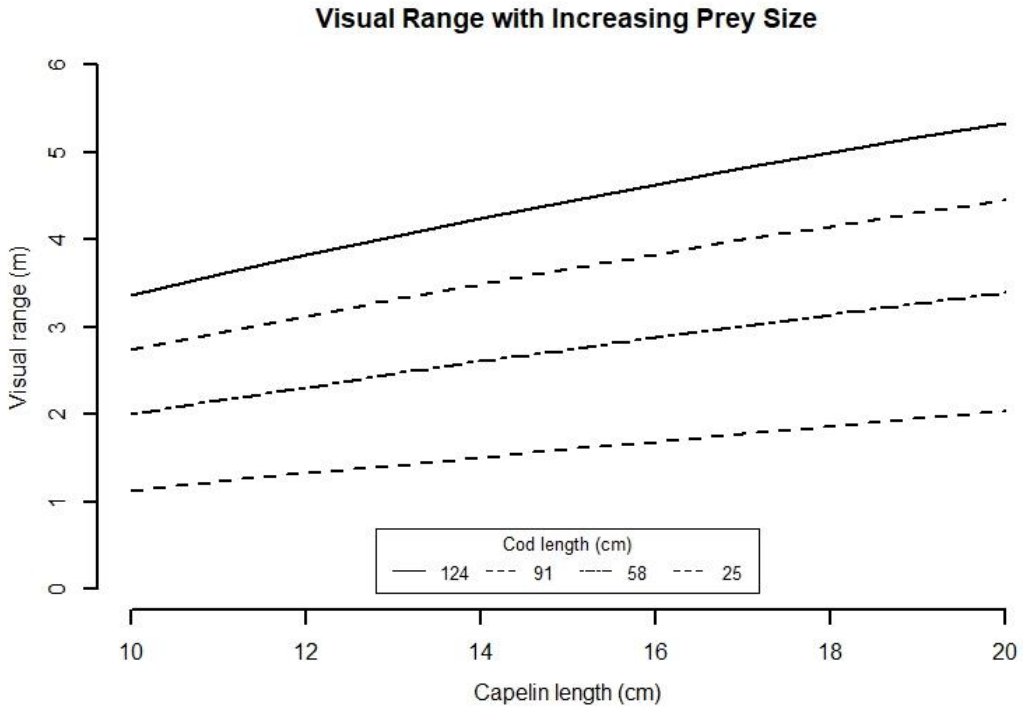

Figure A2. The visual range for four different cod sizes over a range of different capelin sizes. Light levels are congruent with 195 m depth for all cod lengths.

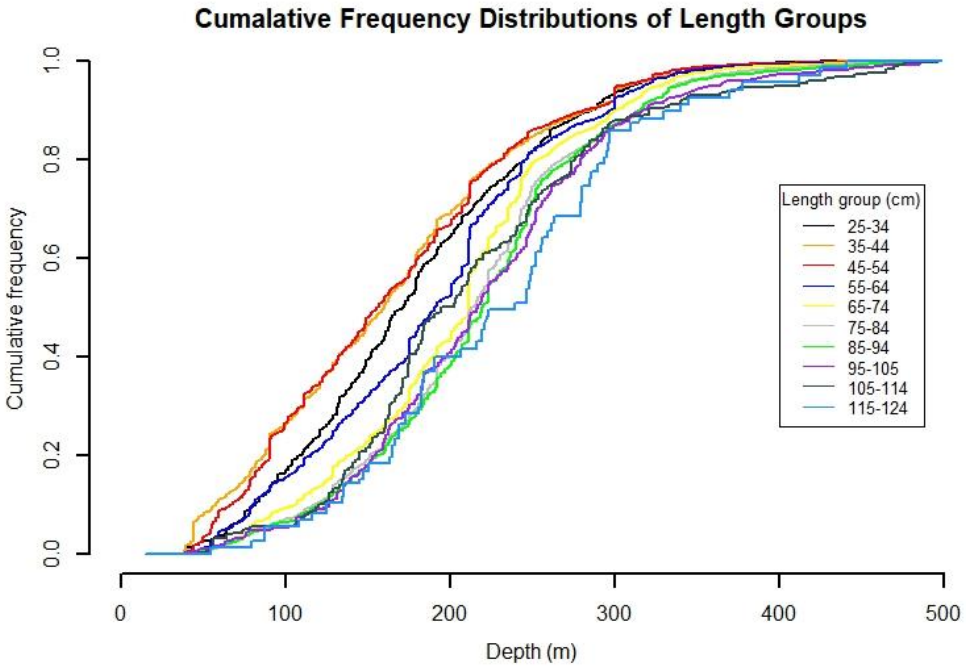

Figure A3. The cumulative frequency distribution of the different length groups, showing at which depths a certain amount of the catch has been made.

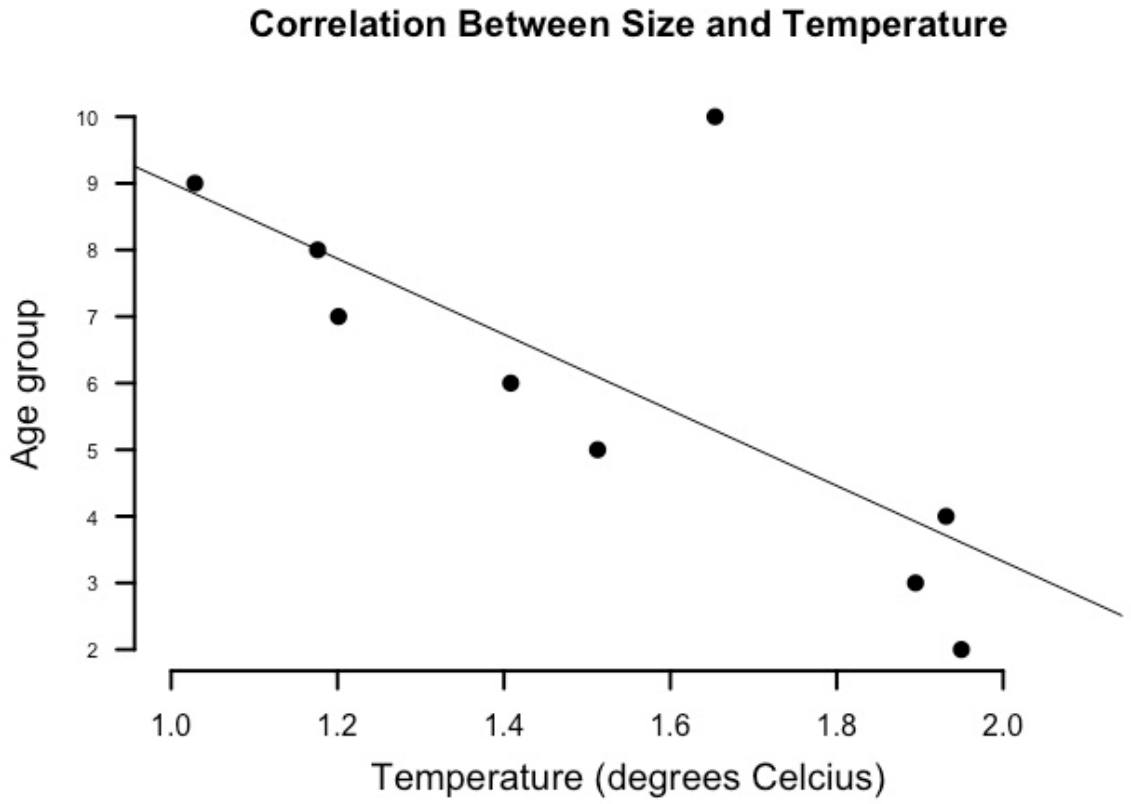

Figure A4. The average temperature for different age groups show a preference for colder waters as size increases.

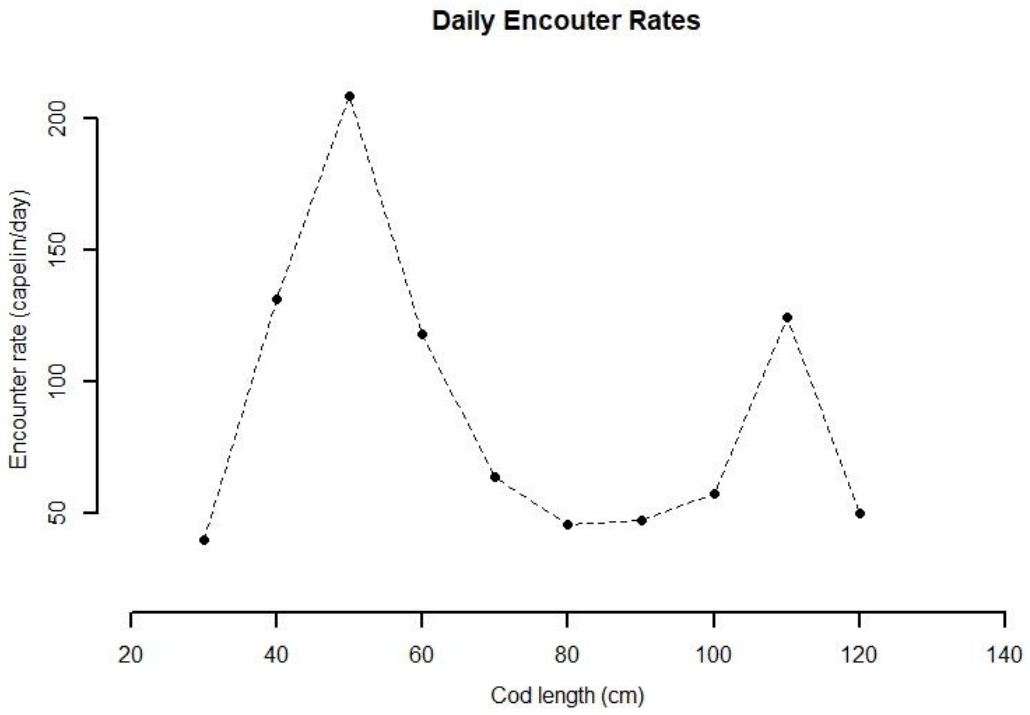

Figure A5. The calculated daily encounter rates for each length group at their respective average depth.

8. Appendix 2 - Optical Structure in Teleosts

Teleosts, being such a large group of vertebrates provide a huge diversity with regards to visual adaptations (Bowmaker, 2008.) Vision based hunting faces bigger limitations in water than on land, as water absorbs and scatters light to a much higher degree than air. Still, most fish species rely heavily on visual ques for orientation and hunting, at least in the mesopelagic part of the ocean (Kotrschal, Van Staaden and Huber, 1998.) Light levels in the top 1000 m of the ocean is sufficient to allow predators to hunt for prey relying mainly on eyesight (Gagnon, Sutton and Johnsen, 2015.)

The lens in most fishes is the only structure responsible for producing an image on the retina (Jagger, 1992.) The immersion in water renders the cornea ineffective, simplifying the design of the fish eye. However, unlike terrestrial animals, they do not get the added benefit of the air/cornea interface with regards to dioptric strength. In humans, this interface provides 43 diopters of refractive power (in contrast, the lens provides 13) which means the human eye loses almost 80 % of its refractive power once it is submerged (Douglas & Djamgoz, 1990).

Hence, a fish eye lens needs to be more powerful without becoming too large. This has led to the spherical shape of most teleost lenses, with a few exceptions (some specialized fish that hunt in the air/water interface like four-eyed minnows (*Anableps sp.*) have developed non-spherical lenses, due to the different requirements imposed by the two elements (Collin and Marshall, 2003.)) The spherical shape of the lens produces another problem; aberration. (Gagnon, Sutton and Johnson, 2015.) A spherical glass ball of uniform refractive index would produce a fair amount of chromatic aberration. Most fish probably combat this by having a lens with an increasing refractive index when moving from the lens cortex to the core (Jagger, 1992.) The spherical shape of the fish lens, necessary for creating a sharp image of the surrounding environment, means that accommodation is achieved by changing the distance between the lens and the retina (Schwassmann, 1975.) This differs from the eyes of say humans, where accommodation is attained by changing the curvature of the lens and thus its refractive power.

The lens is of course not the only a part of the visual system and is by no means the single, or even the principal, contributor to a species visual acuity or light sensitivity. Most teleost´s are equipped with a duplex retina, enabling them to see well at both high and low irradiance levels (Munz & McFarland, 1977.) The scotopic system, based on the photoreceptors known as rods, is responsible for providing most of the information sent to the brain in low light conditions. Contrary, the photopic system (cones) is responsible for most of the visual information during high levels of light intensity. The photopic system also allows the differentiation of wavelengths, allowing for some sort of color vision and most mature teleost´s are believed to be tri- or at least dichromatic. In most teleost´s, the pupil is a fixed size. This prevents them from using it as an aperture, a common feature restricting the amount of light that reaches the retina in most other vertebrates. To be able to cope with intense light conditions they have evolved photoreceptors and shielding pigments (in the retinal pigment epithelium) both capable of "photomechanical" movements (Munz & McFarland, 1977.) This is done to shield the photosensitive rods from potentially damaging light intensities. For a comprehensive study on the cones and rods in fish, see "The Visual Pigments of Fish" (Bowmaker, 1995.)

9. Appendix 3 - R script

Script for Figure 3 and Linear Modell

```
BL.df<-read.table("BLvsLR.csv", header=T, sep=";", dec=",")

Body_length<-BL.df$BL

Lens_radius<-BL.df$LR

lens_radius2<-c(2.9, 4.4)

Length2<-c(27, 52)

plot(lens_radius2~Length2, pch=2 ,xlab="", ylab="", main="Relationship Between Body Length and Lens Radius", cex.main=1.25, axes=F, xlim=c(20,90), ylim=c(2,8))

points(Lens_radius~Body_length, col="black", pch=16)

axis(1,lwd=2)

axis(2,lwd=2)

mtext(text = "Lens radius (mm)", side = 2, line =2.5 , font.lab=2, cex=1)

mtext(text = "Body length (cm)", side = 1, line =2.5 , font.lab=2, cex=1)

abline(lm(Lens_radius~Body_length))

abline(lm(lens_radius2~Length2), lty=3,  col="darkgrey")

lm(formula = Lens_radius~Body_length)

fit1 <- lm(Lens_radius~Body_length)

summary(fit1)
```

Script for Figure 4

```
LW.df<-read.table("Length_weight_IMR.csv", header=T, sep=";", dec=",")

L<-LW.df$length

W<-LW.df$weight
```

```
plot(W~L, xlab="", ylab="",  pch=1, col="midnightblue", main="Relationship Between Length and Weight for the NEAC", cex.main=1.25, axes=F, xlim=c(20,150), ylim=c(100, 25000))

axis(1,lwd=2)

axis(2,lwd=2)

mtext(text = "Weight (g)", side = 2, line =2.5 , font.lab=2, cex=1)

mtext(text = "Length (cm)", side = 1, line =2.5 , font.lab=2, cex=1)
```

Script for Figure 5

```
NRG.df<-read.table("EncR weighted.csv", header=T, sep=";", dec=",")

head(NRG.df)

SMR<-NRG.df$Daily.SMR

W<-NRG.df$Weight

plot(SMR~W, log="x", col="black", lty=1, type="l", lwd=3, ylab="", xlab="", main="Daily Energy Requirements", xlim=c(100,20000), ylim=c(0,250), axes=F)

axis(1,lwd=2)

axis(2,lwd=2)

mtext(text = "Daily energy requirement (kJ/day)", side = 2, line =2.5 , font.lab=2, cex=1)

mtext(text = "Cod weight (g)", side = 1, line =2.5 , font.lab=2, cex=1)
```

Script for Figure 6

```
torsk_l<-read.table("RAWdataII.csv",header=T,sep=";",dec=",")

names(torsk_l)

par(mfrow=c(1,1))

plot(dw1, xlab="", ylab="", main="Length Group 25-34 cm", ylim=c(0,0.007), axes=F)

polygon(d, col = "grey")

lines(dw1, lwd=3, col="darkorchid4")

axis(1,lwd=2)
```

```
axis(2,lwd=2)
mtext(text = "Probability", side = 2, line =2.5 , font.lab=2, cex=1.25)
mtext(text = "Depth (m)", side = 1, line =2.5 , font.lab=2, cex=1.25)

plot(dw2, xlab="", ylab="", main="Length Group 35-44 cm", ylim=c(0,0.007), axes=F)
polygon(d, col = "grey")
lines(dw2, lwd=3, col="midnightblue")
axis(1,lwd=2)
axis(2,lwd=2)
mtext(text = "Probability", side = 2, line =2.5 , font.lab=2, cex=1.25)
mtext(text = "Depth (m)", side = 1, line =2.5 , font.lab=2, cex=1.25)

plot(dw3, xlab="", ylab="", main="Length Group 45-54 cm", ylim=c(0,0.007), axes=F)
polygon(d, col = "grey")
lines(dw3, lwd=3, col="royalblue4")
axis(1,lwd=2)
axis(2,lwd=2)
mtext(text = "Probability", side = 2, line =2.5 , font.lab=2, cex=1.25)
mtext(text = "Depth (m)", side = 1, line =2.5 , font.lab=2, cex=1.25)

plot(dw4, xlab="", ylab="", main="Length Group 55-64 cm", ylim=c(0,0.007), axes=F)
polygon(d, col = "grey")
lines(dw4, lwd=3, col="darkgreen")
axis(1,lwd=2)
axis(2,lwd=2)
mtext(text = "Probability", side = 2, line =2.5 , font.lab=2, cex=1.25)
```

```
mtext(text = "Depth (m)", side = 1, line =2.5 , font.lab=2, cex=1.25)

plot(dw5, xlab="", ylab="", main="Length Group 65-74 cm", ylim=c(0,0.007), axes=F)
polygon(d, col = "grey")
lines(dw5, lwd=3, col="green4")
axis(1,lwd=2)
axis(2,lwd=2)
mtext(text = "Probability", side = 2, line =2.5 , font.lab=2, cex=1.25)
mtext(text = "Depth (m)", side = 1, line =2.5 , font.lab=2, cex=1.25)

plot(dw6, xlab="", ylab="", main="Length Group 75-84 cm", ylim=c(0,0.007), axes=F)
polygon(d, col = "grey")
lines(dw6, lwd=3, col="gold4")
axis(1,lwd=2)
axis(2,lwd=2)
mtext(text = "Probability", side = 2, line =2.5 , font.lab=2, cex=1.25)
mtext(text = "Depth (m)", side = 1, line =2.5 , font.lab=2, cex=1.25)

plot(dw7, xlab="", ylab="", main="Length Group 85-94 cm", ylim=c(0,0.007), axes=F)
polygon(d, col = "grey")
lines(dw7, lwd=3, col="orange4")
axis(1,lwd=2)
axis(2,lwd=2)
mtext(text = "Probability", side = 2, line =2.5 , font.lab=2, cex=1.25)
mtext(text = "Depth (m)", side = 1, line =2.5 , font.lab=2, cex=1.25)
```

```
plot(dw8, xlab="", ylab="", main="Length Group 95-104 cm", ylim=c(0,0.007), axes=F)
polygon(d, col = "grey")
lines(dw8, lwd=3, col="darkorange4")
axis(1,lwd=2)
axis(2,lwd=2)
mtext(text = "Probability", side = 2, line =2.5 , font.lab=2, cex=1.25)
mtext(text = "Depth (m)", side = 1, line =2.5 , font.lab=2, cex=1.25)

plot(dw9, xlab="", ylab="", main="Length Group 105-114 cm", ylim=c(0,0.007), axes=F)
polygon(d, col = "grey")
lines(dw9, lwd=3, col="red4")
axis(1,lwd=2)
axis(2,lwd=2)
mtext(text = "Probability", side = 2, line =2.5 , font.lab=2, cex=1.25)
mtext(text = "Depth (m)", side = 1, line =2.5 , font.lab=2, cex=1.25)

plot(dw10, xlab="", ylab="", main="Length Group 115-124 cm", ylim=c(0,0.007), axes=F)
polygon(d, col = "grey")
lines(dw10, lwd=3, col="darkred")
axis(1,lwd=2)
axis(2,lwd=2)
mtext(text = "Probability", side = 2, line =2.5 , font.lab=2, cex=1.25)
mtext(text = "Depth (m)", side = 1, line =2.5 , font.lab=2, cex=1.25)
```

Script for Figure 7 and Linear Model

```
torsk_l<-read.table("RAWdataII.csv",header=T,sep=";",dec=",")
```

```
wml1<-weighted.mean(torsk_l$Depth, torsk_l$X25.34) #vektet snitt hver stasjon er vektet med antall torsk i den aldersgruppa i stasjonen

wml2<-weighted.mean(torsk_l$Depth, torsk_l$X35.44)

wml3<-weighted.mean(torsk_l$Depth, torsk_l$X45.54)

wml4<-weighted.mean(torsk_l$Depth, torsk_l$X55.64)

wml5<-weighted.mean(torsk_l$Depth, torsk_l$X65.74)

wml6<-weighted.mean(torsk_l$Depth, torsk_l$X75.84)

wml7<-weighted.mean(torsk_l$Depth, torsk_l$X85.94)

wml8<-weighted.mean(torsk_l$Depth, torsk_l$X95.104)

wml9<-weighted.mean(torsk_l$Depth, torsk_l$X105.114)

wml10<-weighted.mean(torsk_l$Depth, torsk_l$X115.124)

length<-seq(1,10, by=1)

dyp<- c(wml1,wml2,wml3,wml4,wml5,wml6,wml7,wml8,wml9,wml110)

test<-lm(dyp~length)

summary(test)

plot(dyp~length, pch = 16, cex = 1.3, col = "black", main = "Average Depth for Length Groups", xlab = "", ylab = "", cex.main=1.25, xlim=c(0,10), ylim=rev(c(160,240)), axes=F)

text(1,177, "177", pos=3)

text(2,163, "163", pos=3)

text(3,164, "164", pos=3)

text(4,188, "188", pos=3)

text(5,204, "204", pos=3)

text(6,214, "214", pos=3)

text(7,217, "217", pos=3)

text(8,219, "219", pos=3)

text(9,213, "213", pos=3)

text(10,230, "230", pos=3)
```

```
axis(2,lwd=2)

axis(1, lwd=2, cex.axis=0.7, las=1, at=1:10, labels=c("25-34", "35-44","45-54","55-64","65-74","75-84","85-94", "95-104","105-114","115-124"))

abline(lm(dyp~length))

mtext(text = "Length groups (cm)", side = 1, line =3 , font.lab=2, cex=1)

mtext(text = "Depth (m)", side = 2, line =2.5 , font.lab=2, cex=1)
```

Script for Figure 8

```
modell1.df<-read.table("Bok1.csv",header=T,sep=";",dec=",")

head(modell1.df)

LR<-modell1.df$Lens.radius

VR<-modell1.df$Visual.range

Le<-modell1.df$Length

VRnoc<-modell1.df$VisR

plot(VR~LR, xlab="", ylab="", col="black", pch=20, main="Relationship Between Lens Radius and Visual Range", cex.main=1.25, axes=F, xlim=c(2,10), ylim=c(1,5.5))

lines(VRnoc~LR, lty=2, col="darkgrey")

axis(1,lwd=2)

axis(2,lwd=2)

mtext(text = "Visual range (m)", side = 2, line =2.5 , font.lab=2, cex=1)

mtext(text = "Lens radius (mm)", side = 1, line =2.5 , font.lab=2, cex=1)
```

Script for Figure 9, panel A

```
EncR.df<-read.table("EncR weighted.csv", header=T, sep=";", dec=",")

LG<-EncR.df$Length.1

VisR<-EncR.df$VisR.at.depth
```

```
SV<-EncR.df$Search.volume.1

par(mar = c(5,5,2,5))

plot(SV~LG, col="black", cex = 1, ylab="", pch=16, xlab="", main="Visual Range and
Search Volume", xlim=c(20,140), ylim=c(2000,45000), axes=F)

lines(SV~LG, lty=6, pch = 16, cex = 1, col = "black")

axis(1,lwd=2)

axis(2,lwd=2)

text(30,8469, "177", cex=0.7, pos=1)

text(40,27998, "163", cex=0.7, pos=4)

text(50,44398, "164", cex=0.7, pos=3)

text(60,25143, "188", cex=0.7, pos=4)

text(70,13437, "204", cex=0.7, pos=4)

text(80,9732, "214", cex=0.7, pos=3)

text(90,10023, "217", cex=0.7, pos=1)

text(100,12279, "219", cex=0.7, pos=1)

text(110,26498, "213", cex=0.7, pos=3)

text(120,10614, "230", cex=0.7, pos=1)

mtext(text = "Search volume (m^3/hour)", side = 2, line =2.5 , font.lab=2, cex=1)

mtext(text = "Cod length (cm)", side = 1, line =2.5 , font.lab=2, cex=1)

par(new = T)

plot(VisR~LG, col = "deepskyblue4", pch = 16,  ylab="", xlab="", ylim=c(1,3.7),
xlim=c(20,140), axes=F)

lines(VisR~LG, lty=4, pch = 16, cex = 1, col = "deepskyblue4")

legend(65, 3.5, legend=c("Search volume","Visual range"),pch=c(16,16), lty=c(6,4),
col=c("black", "deepskyblue4"), cex=0.8, box.lty=1)

axis(4, lwd=2)

mtext(text = "Visual range (m)", side = 4, line =2.5 , font.lab=2, cex=1)
```

Script for Figure 9, panel B

```
EncR.df<-read.table("EncR weighted.csv", header=T, sep=";", dec=",")

LG<-EncR.df$Length.1

DER<-EncR.df$DER

SMR<-EncR.df$SMR

VisR<-EncR.df$VisR.at.depth

SV<-EncR.df$Search.volume.1

EncRW<-NRG.df$EncR.W

par(mar = c(5,5,2,5))

plot(EncRW~LG, col="black", cex = 1, ylab="", pch=16, xlab="", main="Visual Range and Spesific Encounter Rates", xlim=c(20,140), ylim=c(0,0.3), axes=F)

lines(EncRW~LG, lty=6, pch = 16, cex = 1, col = "black")

axis(1,lwd=2)

axis(2,lwd=2)

mtext(text = "Specific encounter rates (kJ/day/g)", side = 2, line =2.5 , font.lab=2, cex=1)

mtext(text = "Cod length (cm)", side = 1, line =2.5 , font.lab=2, cex=1)

par(new = T)

plot(VisR~Length, col="deepskyblue4", cex = 1, ylab="", pch=16, xlab="", xlim=c(20,140), ylim=c(1,3.7), axes=F)

lines(VisR~Length, lty=4, pch = 16, cex = 1, col = "deepskyblue4")

legend(65, 3.5, legend=c("Specific encounter rates","Visual range"),pch=c(16,16), lty=c(6,4), col=c("black","deepskyblue4"), cex=0.8, box.lty=1)

axis(4, lwd=2)

mtext(text = "Visual range (m)", side = 4, line =2.5 , font.lab=2, cex=1)
```

Script for Figure 9, panel C

```
EncR.df<-read.table("EncR weighted.csv", header=T, sep=";", dec=",")

SMR<-EncR.df$SMR
```

```
LG<-EncR.df$Length.1

kJ<-NRG.df$KJ.from.encounters

par(mar = c(5,5,2,5))

plot(kJ~LG, col="black", cex = 1, ylab="", pch=16, xlab="", main="Daily Energy Encounter Rates and SMR", xlim=c(20,140), ylim=c(1000,9000), axes=F)

lines(kJ~LG, lty=6, pch = 16, cex = 1, col = "black")

axis(1,lwd=2)

axis(2,lwd=2)

mtext(text = "Encountered energy(kJ/day)", side = 2, line =2.5 , font.lab=2, cex=1)

mtext(text = "Cod length (cm)", side = 1, line =2.5 , font.lab=2, cex=1)

par(new = T)

plot(SMR~Length, col="deepskyblue4", cex = 1, ylab="", pch=16, xlab="", xlim=c(20,140), ylim=c(5,205), axes=F)

lines(SMR~Length, lty=4, pch = 16, cex = 1, col = "deepskyblue4")

legend(65, 200, legend=c("Encountered energy","SMR"),pch=c(16,16), lty=c(6,4), col=c("black", "deepskyblue4"), cex=0.8, box.lty=1)

axis(4, lwd=2)

mtext(text = "SMR (kJ/day)", side = 4, line =2.5 , font.lab=2, cex=1)
```

Script for Figure 9, panel D

```
NRG.df<-read.table("EncR weighted.csv", header=T, sep=";", dec=",")

head(NRG.df)

Length<-NRG.df$Length.1

Netto<-NRG.df$Netto.NRG

EncRW<-NRG.df$EncR.W

par(mar = c(5,5,2,5))

plot(Netto~Length, pch=16, col="black",  ylab="", xlab="", main="Daily Specific Encounter Rates and Netto Energy Balance", xlim=c(20,140), ylim=c(0,10), axes=F)
```

```
lines(Netto~Length, lty=6, pch = 16, cex = 1, col = "black")

axis(1,lwd=2)

axis(2,lwd=2)

mtext(text = "Specific energy balance (kJ/g)", side = 2, line =2.5 , font.lab=2, cex=1)

mtext(text = "Cod length (cm)", side = 1, line =2.5 , font.lab=2, cex=1)

par(new = T)

plot(EncRW~Length, col="deepskyblue4", cex = 1, ylab="", pch=16, xlab="",
xlim=c(20,140), ylim=c(0.001,0.3), axes=F)

lines(EncRW~Length, lty=4, pch = 16, cex = 1, col = "deepskyblue4")

legend(65, 0.29, legend=c("Specific energy balance","Specific encounter
rate"),pch=c(16,16), lty=c(6,4), col=c("black", "deepskyblue4"), cex=0.8, box.lty=1)

axis(4, lwd=2)

mtext(text = "Specific encounter rate (capelin/day/g)", side = 4, line =2.5 , font.lab=2,
cex=1)
```

Script for Figure A1

```
temp.df<-read.table("temp_depthII.csv",header=T,sep=";",dec=",")

Bathymetric<-
c(50,60,70,80,90,100,110,120,130,140,150,160,170,180,190,200,210,220,230,240,250,260,270
,280,290,300,310,320,330,340,350,360,370,380,390,400,410,420,430,440,450,460,470,4
80,490)

mntemp50<-mean(temp.df$Bathy__50, na.rm = TRUE)

mntemp60<-mean(temp.df$Bathy__60, na.rm = TRUE)

mntemp70<-mean(temp.df$Bathy__70, na.rm = TRUE)

mntemp80<-mean(temp.df$Bathy__80, na.rm = TRUE)

mntemp90<-mean(temp.df$Bathy__90, na.rm = TRUE)

mntemp100<-mean(temp.df$Bathy__100, na.rm = TRUE)

mntemp110<-mean(temp.df$Bathy__110, na.rm = TRUE)

mntemp120<-mean(temp.df$Bathy__120, na.rm = TRUE)
```

```
mntemp130<-mean(temp.df$Bathy__130, na.rm = TRUE)
mntemp140<-mean(temp.df$Bathy__140, na.rm = TRUE)
mntemp150<-mean(temp.df$Bathy__150, na.rm = TRUE)
mntemp160<-mean(temp.df$Bathy__160, na.rm = TRUE)
mntemp170<-mean(temp.df$Bathy__170, na.rm = TRUE)
mntemp180<-mean(temp.df$Bathy__180, na.rm = TRUE)
mntemp190<-mean(temp.df$Bathy__190, na.rm = TRUE)
mntemp200<-mean(temp.df$Bathy__200, na.rm = TRUE)
mntemp210<-mean(temp.df$Bathy__210, na.rm = TRUE)
mntemp220<-mean(temp.df$Bathy__220, na.rm = TRUE)
mntemp230<-mean(temp.df$Bathy__230, na.rm = TRUE)
mntemp240<-mean(temp.df$Bathy__240, na.rm = TRUE)
mntemp250<-mean(temp.df$Bathy__250, na.rm = TRUE)
mntemp260<-mean(temp.df$Bathy__260, na.rm = TRUE)
mntemp270<-mean(temp.df$Bathy__270, na.rm = TRUE)
mntemp280<-mean(temp.df$Bathy__280, na.rm = TRUE)
mntemp290<-mean(temp.df$Bathy__290, na.rm = TRUE)
mntemp300<-mean(temp.df$Bathy__300, na.rm = TRUE)
mntemp310<-mean(temp.df$Bathy__310, na.rm = TRUE)
mntemp320<-mean(temp.df$Bathy__320, na.rm = TRUE)
mntemp330<-mean(temp.df$Bathy__330, na.rm = TRUE)
mntemp340<-mean(temp.df$Bathy__340, na.rm = TRUE)
mntemp350<-mean(temp.df$Bathy__350, na.rm = TRUE)
mntemp360<-mean(temp.df$Bathy__360, na.rm = TRUE)
mntemp370<-mean(temp.df$Bathy__370, na.rm = TRUE)
mntemp380<-mean(temp.df$Bathy__380, na.rm = TRUE)
```

```
mntemp390<-mean(temp.df$Bathy__390, na.rm = TRUE)

mntemp400<-mean(temp.df$Bathy__400, na.rm = TRUE)

mntemp410<-mean(temp.df$Bathy__410, na.rm = TRUE)

mntemp420<-mean(temp.df$Bathy__420, na.rm = TRUE)

mntemp430<-mean(temp.df$Bathy__430, na.rm = TRUE)

mntemp440<-mean(temp.df$Bathy__440, na.rm = TRUE)

mntemp450<-mean(temp.df$Bathy__450, na.rm = TRUE)

mntemp460<-mean(temp.df$Bathy__460, na.rm = TRUE)

mntemp470<-mean(temp.df$Bathy__470, na.rm = TRUE)

mntemp480<-mean(temp.df$Bathy__480, na.rm = TRUE)

mntemp490<-mean(temp.df$Bathy__490, na.rm = TRUE)


depth<-seq(50,490, by=10)

Temp<-c(mntemp50, mntemp60, mntemp70, mntemp80, mntemp90, mntemp100,
mntemp110, mntemp120, mntemp130, mntemp140, mntemp150, mntemp160,
mntemp170, mntemp180, mntemp190, mntemp200, mntemp210, mntemp220,
mntemp230, mntemp240, mntemp250, mntemp260, mntemp270, mntemp280,
mntemp290, mntemp300, mntemp310, mntemp320, mntemp330, mntemp340,
mntemp350, mntemp360, mntemp370, mntemp380, mntemp390, mntemp400,
mntemp410, mntemp420, mntemp430, mntemp440, mntemp450, mntemp460,
mntemp470, mntemp480, mntemp490)

test<-lm(depth~Temp)

summary(test)

plot(Temp~depth, pch = 16, cex = 1, col = "black", main = "Temperature at Different Depths
in the Barents Sea", xlab = "", ylab = "", cex.main=1.25, xlim=c(0,490), ylim=c(1, 3), axes=F)

axis(1,lwd=2)

axis(2,lwd=2)

mtext(text = "Temperature (degrees Celsius)", side = 2, line =2.5 , font.lab=2, cex=1)

mtext(text = "Depth (m)", side = 1, line =2.5 , font.lab=2, cex=1)
```

```
lines(Temp~depth, col = "black", main = "Correlation Between Depth and Temperature",
xlab = "", ylab = "", cex.main=1.25, xlim=c(0,490), ylim=c(1, 3))

abline(v=c(150,250), col=c("darkgrey", "darkgrey"), lty=c(2,2), lwd=c(1, 1))
```

Script for Figure A2

```
PS.df<-read.table("Searchlength MysCap.csv", header=T, sep=";", dec=",")

head(PS.df)

LC2<-PS.df$X25.cm

LC5<-PS.df$X58.cm

LC9<-PS.df$X91.cm

LC12<-PS.df$X124.cm

Cap<-PS.df$Ap

plot(LC12~Cap, type="l", lwd=2, ylab="", xlab="", main="Visual Range with Increasing
Prey Size", ylim=c(0,6), xlim=c(10, 20), axes=F)

lines(LC9~Cap, lty=2, lwd=2)

lines(LC5~Cap, lty=6, lwd=2)

lines(LC2~Cap, lty=8, lwd=2)

axis(1,lwd=2)

axis(2,lwd=2)

legend(12.8,0.7, legend=c("124","91", "58", "25"),

    title="Cod length (cm)",lty=c(1,2,6,8), cex=0.8, box.lty=1, ncol=4)

mtext(text = "Visual range (m)", side = 2, line =2.5 , font.lab=2, cex=1)

mtext(text = "Capelin length (cm)", side = 1, line =2.5 , font.lab=2, cex=1)
```

Script for Figure A3

```
Var.df<-read.table("Variation.csv",header=T,sep=";",dec=",")

head(Var.df)

dep<-Var.df$ï..Depth

lg1<-Var.df$X25.34

lg2<-Var.df$X35.44

lg3<-Var.df$X45.54

lg4<-Var.df$X55.64

lg5<-Var.df$X65.74

lg6<-Var.df$X75.84

lg7<-Var.df$X85.94

lg8<-Var.df$X95.104

lg9<-Var.df$X105.114

lg10<-Var.df$X115.124

par(mar = c(5,5,2,5))

plot(lg1~dep, lty=1, type="l", lwd=2, cex = 1.3, col = "black", main = "Cumalative Frequency Distributions of Length Groups", cex.main=1.25, xlab = "", ylab = "",  ylim=c(0,1), xlim=c(0,500), axes=F)

axis(2,lwd=2)

axis(1, lwd=2) #cex.axis=0.7, las=1, at=0:10, labels=c("10", "20","30","40","50","60","70", "80","90","100"))

mtext(text = "Depth (m)", side = 1, line =2.5 , font.lab=2, cex=1)

mtext(text = "Cumulative frequency", side = 2, line =2.5 , font.lab=2, cex=1)

par(new=T)

plot(lg2~dep, lty=1, type="l", lwd=2, cex = 1.3, col = "orange",  xlab = "", ylab = "", ylim=c(0,1), xlim=c(0,500), axes=F)
```

```
par(new=T)

plot(lg3~dep, lty=1, type="l", lwd=2, cex = 1.3, col = "red",  xlab = "", ylab = "", ylim=c(0,1),
xlim=c(0,500), axes=F)


par(new=T)

plot(lg4~dep, lty=1, type="l", lwd=2, cex = 1.3, col = "blue",  xlab = "", ylab = "", ylim=c(0,1),
xlim=c(0,500), axes=F)


par(new=T)

plot(lg5~dep, lty=1, type="l", lwd=2, cex = 1.3, col = "yellow", xlab = "", ylab = "", ylim=c(0,1),
xlim=c(0,500), axes=F)


par(new=T)

plot(lg6~dep, lty=1, type="l", lwd=2, cex = 1.3, col = "grey", xlab = "", ylab = "",  ylim=c(0,1),
xlim=c(0,500), axes=F)


par(new=T)

plot(lg7~dep, lty=1, type="l", lwd=2, cex = 1.3, col = "green", xlab = "", ylab = "", ylim=c(0,1),
xlim=c(0,500), axes=F)


par(new=T)

plot(lg8~dep, lty=1, type="l", lwd=2, cex = 1.3, col = "purple", xlab = "", ylab = "",  ylim=c(0,1),
xlim=c(0,500), axes=F)


par(new=T)

plot(lg9~dep, lty=1, type="l", lwd=2, cex = 1.3, col = "darkslategrey", xlab = "", ylab = "",
ylim=c(0,1), xlim=c(0,500), axes=F)
```

```
par(new=T)

plot(lg10~dep, lty=1, type="l", lwd=2, cex = 1.3, col = "dodgerblue", xlab = "", ylab = "",
ylim=c(0,1), xlim=c(0,500), axes=F)


legend(400,0.75, legend=c("25-34","35-44","45-54","55-64","65-74", "75-84", "85-94",
"95-105", "105-114", "115-124"), col=c("black", "orange", "red", "blue", "yellow", "grey",
"green", "purple", "darkslategrey", "dodgerblue"), title="Length group (cm)", lty=1:1,
cex=0.8)
```

Script for Figure A4

```
setwd("~/Documents/Master")

torsk_T<-read.table("MagedataIII.csv",header=T,sep=";",dec=",")

#wml1<-weighted.mean(torsk_T$Temperature, torsk_T$age__1)

wml2<-weighted.mean(torsk_T$Temperature, torsk_T$age__2)

wml3<-weighted.mean(torsk_T$Temperature, torsk_T$age__3)

wml4<-weighted.mean(torsk_T$Temperature, torsk_T$age__4)

wml5<-weighted.mean(torsk_T$Temperature, torsk_T$age__5)

wml6<-weighted.mean(torsk_T$Temperature, torsk_T$age__6)

wml7<-weighted.mean(torsk_T$Temperature, torsk_T$age__7)

wml8<-weighted.mean(torsk_T$Temperature, torsk_T$age__8)

wml9<-weighted.mean(torsk_T$Temperature, torsk_T$age__9)

wml10<-weighted.mean(torsk_T$Temperature, torsk_T$age_10)

lengde<-seq(2,10, by=1)

Temp<-c(wml2,wml3,wml4,wml5,wml6,wml7,wml8,wml9, wml10)

test<-lm(lengde~Temp)

summary(test)

plot(lengde~Temp, pch = 16, cex = 1.3, col = "black", main = "Correlation Between Size
and Temperature", xlab = "", ylab = "", cex.main=1.25, xlim=c(1,2.1), ylim=c(2, 10), axes=F)
```

```
axis(1,lwd=2)

axis(2, lwd=2, cex.axis=0.7, las=1, at=2:10)

abline(lm(lengde~Temp))

mtext(text = "Age group", side =2, line =2.5 , font.lab=2, cex=1)

mtext(text = "Temperature (degrees Celcius)", side = 1, line =2.5 , font.lab=2, cex=1)
```

Script for Figure A5

```
EncR.df<-read.table("EncR weighted.csv", header=T, sep=";", dec=",")

head(EncR.df)

tail(EncR.df)

LG<-EncR.df$Length.1

print(LG)

L<-EncR.df$Length

DER<-EncR.df$DER.1

print(DER)

SMR<-EncR.df$Daily.SMR

VisR<-EncR.df$VisR.at.depth

ERE<-EncR.df$Energy.needs.encounter


par(mar = c(5,5,2,5))

plot(DER~LG, col="black", ylab="", pch=16, xlab="", main="Daily Encouter Rates",
xlim=c(20,140), ylim=c(20,220), axes=F)

lines(DER~LG, lty=2, pch = 16, cex = 1, col = "black")

axis(1,lwd=2)

axis(2,lwd=2)
```